The Electric Field Gradient at the Site of the Halogen Ion and Structure of Amino Acid Hydrobromides and Hydroiodides

Armin Kehrer, Shi-qi Dou, and Alarich Weiss

Institut für Physikalische Chemie, Physikalische Chemie III, Technische Hochschule Darmstadt, Darmstadt, Germany

Z. Naturforsch. **47a**, 887–917 (1992); received January 16, 1992

The ^{79,81}Br and ^{127}I NQR spectra of several hydrobromides, respectively hydroiodides, of amino acides and dipeptides were studied, mostly as functions of temperature in the range $77 \leq T/\mathrm{K} \leq 420$. The investigated compounds are: L-Arg · HBr · H_2O, L-Cys · HBr · H_2O, L-Cys–S–S–L–Cys · 2 HBr, ethanolamine · HBr, L-Glu · HBr, L-His · HBr, L-His · 2 HBr, L-Ile · HBr · H_2O, Sar · HBr, $(Sar)_2$ · HBr, L-Val · HBr · H_2O, Gly · LiBr, Gly-Gly · LiBr, ethanolamine · HI, Sar · HI, $(Sar)_2$ · HI, $(Gly)_2$ · HI, $(L\text{-Val})_2$ · HI, Gly-L-Leu · HI · H_2O. A phase transition with hysteresis was observed for L-Val · HBr · H_2O ($T_{c,up} = 318$ K, $T_{c,down} = 242$ K). Two solid phases of Sar · HI have been studied by NQR, one crystallized from melt, the other one from aqueous solution.

For three of the title compounds the crystal structure was determined at room temperature: L-His · 2 HBr, $P2_12_12_1$, $Z=4$, $a/\mathrm{pm} = 1652$, $b/\mathrm{pm} = 916$, $c/\mathrm{pm} = 721$; L-Cys · HBr · H_2O, $P2_12_12_1$, $Z=4$, $a/\mathrm{pm} = 1955$, $b/\mathrm{pm} = 746$, $c/\mathrm{pm} = 550$; Gly-L-Leu · HI · H_2O, $P2_1$, $Z=2$, $a/\mathrm{pm} = 1289$, $b/\mathrm{pm} = 914$, $c/\mathrm{pm} = 615$, $\beta/° = 99$.

In most cases the halogen ion in the studied hydrohalides is polycoordinated by hydrogen bonds of the type N–H ··· $X^{\ominus}$ and O–H ··· $X^{\ominus}$, X = Br, I. The NQR frequencies and, for iodine, the nuclear quadrupole coupling constants depend on this coordination. A low frequency (coupling constant) region is found for pure N–H ··· $X^{\ominus}$ coordination. Replacing one N–H ··· $X^{\ominus}$ bond by O–H ··· $X^{\ominus}$ rises the electric field gradient, EFG, respectively the resonance frequencies.

The dependence of the EFG on the hydrogen bond coordination N–H ··· $X^{\ominus}$ plus O–H ··· $X^{\ominus}$ is discussed for the title compounds including information from literature.

Introduction

Some years ago, Fleck and Weiss [1], in connection with the study of pyroelectric properties of amino acids, proposed a rule for the dependence of ^{79,81}Br nuclear quadrupole resonance (NQR) frequencies on the hydrogen bond coordination of the $Br^{\ominus}$ ion in hydrobromides of amino acids and amines. Upper and lower limits for the ^{79}Br NQR frequencies have been given in dependence on the number and kind of the hydrogen bonds N–H ··· $Br^{\ominus}$ and O–H ··· $Br^{\ominus}$. In compounds, in which $Br^{\ominus}$ experiences bonds N–H ··· $Br^{\ominus}$ only, the ^{79}Br NQR frequencies are observed in the range $12 \leq \nu(^{79}\mathrm{Br})/\mathrm{MHz} \leq 20$ [2]. An additional hydrogen bond O–H ··· $Br^{\ominus}$, however, shifts the ^{79}Br NQR frequency to a higher range, $19.5 \leq \nu(^{79}\mathrm{Br})/\mathrm{MHz} \leq 27.5$ (at $T = 273$ K). The different ranges of the NQR frequencies and, therefore, the different strength of the electric field gradient, EFG, acting at the bromine site, may be explained by the different strength of the hydrogen bonds responsible for the main contribution to the EFG. Hydrogen bonds O–H ··· $Br^{\ominus}$ are stronger than bonds N–H ··· $Br^{\ominus}$ [3] and, therefore, contribute more to the EFG at the site of the bromine nucleus than the latter ones. Additionally, in case of bonds N–H ··· $Br^{\ominus}$ only, the symmetry of the charge distribution around the bromine ion will be higher than in case where one additional O–H ··· $Br^{\ominus}$ is present. Correspondingly, the acting EFG will be higher in the later case.

For amine hydroiodides and amino acid hydroiodides a similar relation between the ^{127}I nuclear quadrupole coupling constant, (NQCC) $e\Phi_{zz}Qh^{-1} = e^2qQh^{-1}$ (e = unit charge, Φ_{zz} = main principal axis of the EFG tensor, eQ = nuclear electric quadrupole moment, h = Planck's constant) and the kind of the hydrogen bond linkages to $I^{\ominus}$ was observed [4].

In the following we report the crystal structures and the halogen NQR spectra of L-histidine dihydrobromide (L-His · 2 HBr), L-cysteine hydrobromide monohydrate (L-Cys · HBr · H_2O), and glycyl-L-leucine hydroiodide monohydrate (Gly-L-Leu · HI · H_2O). The halogen NQR data of several other amino acid hydrohalides are reported, too (without crystal structure investigation; for some of the title compounds the

Reprint requests to Prof. Dr. Al. Weiss, Institut für Physikalische Chemie (III), Technische Hochschule Darmstadt, Petersenstrasse 20, D-6100 Darmstadt.

0932-0784 / 92 / 0700-0887 $ 01.30/0. – Please order a reprint rather than making your own copy.

Table 1. Compounds investigated; abbreviation of the name (short form); habitus, color, melting point (decomposition point in K); chemical analysis (C, H, N, halogen in weight%); property studied.

Compound Short form	Mp/K	Habitus	Color	Chemical analysis (weight%) calc./exp.				Property studied
				C	H	N	X	
L-Arginine hydrobromide monohydrate L-Arg · HBr · H_2O	448*	six sided flat plates	colorless	26.38/26.30	6.27/6.38	20.51/21.06	29.26/29.77	^{79}Br NQR
L-Cysteine hydrobromide monohydrate L-Cys · HBr · H_2O	341*	long thick needles	colorless	16.37/16.30	4.58/4.41	6.36/6.32	36.31/36.39	^{79}Br NQR structure
L-Cystine dihydrobromide L-Cys-S-S-L-Cys · 2 HBr	479*	six sided prisms	colorless, clear	17.92/17.82	3.51/3.51	6.97/6.93	39.74/39.76	^{79}Br NQR
Ethanolamine hydrobromide	361	thick needles	colorless	16.92/16.80	5.68/5.69	9.86/9.86	56.27/56.07	^{79}Br NQR
L-Glutamic acid hydrobromide L-Glu · HBr	483*	six sided thick prisms	colorless	26.33/25.98	4.42/4.05	6.14/6.11	35.04/35.28	^{79}Br NQR
L-Histidine hydrobromide L-His · HBr	513*	large poly-face cryst.	colorless, clear	30.53/30.47	4.27/4.40	17.80/17.12	33.85/34.20	^{79}Br NQR
L-Histidine dihydrobromide L-His · 2 HBr	496	small square plates	colorless, clear	22.73/22.66	3.50/3.37	13.26/13.17	50.42/50.67	^{79}Br NQR structure
L-Isoleucine hydrobromide monohydrate, L-Ile · HBr · H_2O	337	very thin plates	colorless	31.32/30.57	7.01/6.75	6.09/5.84	34.73/35.15	^{79}Br NQR
Sarcosine hydrobromide Sar · HBr	449	thick plates	colorless	21.29/21.13	4.74/4.75	8.24/8.17	47.00/47.22	^{79}Br NQR
Disarcosine hydrobromide $(Sar)_2$ · HBr; slightly hygroscopic	423	long thin needles	colorless	27.81/27.79	5.84/5.85	10.81/10.81	30.84/31.15	^{79}Br NQR
L-Valine hydrobromide monohydrate L-Val · HBr · H_2O; slightly hygroscopic	469	flat plates	colorless	27.79/27.97	6.52/5.58	6.47/6.51	36.98/37.11	^{79}Br NQR
Glycine lithiumbromide Gly · LiBr	508*	long thin needles	colorless	20.27/20.26	4.25/3.69	11.82/12.00	33.72/34.01	^{79}Br NQR
Glycyl-glycine lithiumbromide Gly-Gly · LiBr	508*	six sided prisms	colorless	21.94/21.39	3.68/3.75	12.79/12.67	36.49/36.68	^{79}Br NQR
Ethanolamine hydroiodide	349	thick plates	slightly yellow	12.71/12.62	4.27/4.19	7.41/7.38	67.51/67.57	^{127}I NQR
Sarcosine hydroiodide Sar · HI (from solution)	442	large thin plates	orange	16.60/16.57	3.72/3.66	6.45/6.43	58.48/58.10	^{127}I NQR
Disarcosine hydroiodide $(Sar)_2$ · HI; slightly hygroscopic	419	thin long needles	slightly yellow	23.54/23.60	4.94/4.94	9.15/9.15	41.46/41.69	^{127}I NQR
Diglycine hydroiodide $(Gly)_2$ · HI	421	long thick needles	slightly orange	17.28/17.13	3.99/3.89	10.08/10.04	45.64/45.43	^{127}I NQR
Di-L-Valine hydroiodide $(L\text{-}Val)_2$ · HI	462*	long thick needles	redish	33.16/–	6.12/–	7.73/–	35.07/35.46	^{127}I NQR
Glycyl-L-leucine hydroiodide monohydrate; Gly-L-Leu · HI · H_2O	374	six sided prisms	slightly yellow	28.76/28.64	5.73/5.68	8.38/8.49	37.98/38.17	^{127}I NQR structure

* decomposition.

structures are known). The results are discussed on the basis of the proposed rule about the hydrogen bond and NQR frequency [1, 4], including data available from literature.

Experimental

Preparation

The compounds investigated were prepared from aqueous solutions of commercial amino acids and hydrobromic acid (48%, Aldrich) and hydroiodic acid (57%, Riedel de Haen), respectively. The dipeptide Gly-L-Leu was synthesized according to [5]. The compounds were crystallized from the aqueous solutions (pH: 1–5) by evaporation of the solvent at room temperature or by slow cooling of a saturated solution (in one case also from melt). In Table 1 we list the compounds we deal with here, some of their properties (crystal habitus, color), and the chemical analysis.

Table 2. Experimental conditions in the structure determinations and crystal structure data for L-His · 2 HBr, L-Cys · HBr · H_2O, and Gly-L-Leu · HI · H_2O. Spectrometer: Stoe Stadi-4; wave length: MoKα = 71.069 pm; monochromator: Graphite (002); scan: $\omega/2\vartheta$.

Compound	L-Histidine dihydrobromide, $C_6H_{11}Br_2N_3O_2$	L-Cysteine hydrobromide monohydrate, $C_3H_{10}BrNO_3S$	Glycyl-L-leucine hydroiodide monohydrate, $C_8H_{19}IN_2O_4$
M/(kg · kmol^{-1})	316.99	220.09	335.15
Crystal form,	plates	prism	prism
Size	(0.18 · 0.35 · 0.5) mm^3	(0.2 · 0.35 · 0.9) mm^3	(0.17 · 0.3 · 0.4) mm^3
T/K	297	297	298
Absorption coeff./m^{-1}	7340	5274	2188
(sin ϑ/λ_{max})/pm^{-1}	0.005385	0.006497	0.007035
Number of reflexes measured	1837	4036	4506
Reflexes symmetry independent	1423	1811	4152
Reflexes considered	1382	1796	3979
Number of free parameters	160	113	182
$R(F)$	0.0193	0.0197	0.0226
$R_w(F)$	0.0175	0.0182	0.0213
Lattice constants a/pm	1652.2 (8)	1955.4 (8)	1289.0 (3)
b/pm	915.8 (4)	746.2 (4)	913.7 (2)
c/pm	720.5 (3)	549.5 (3)	615.0 (2)
β/°	90.00	90.00	98.92 (1)
Volume/cell $V \cdot 10^{-6}$/pm	1090.2 (15)	801.7 (12)	715.6 (5)
Space group	D_2^4-P$2_12_12_1$	D_2^4-P$2_12_12_1$	C_2^2-P2_1
Formula unit/cell, Z	4	4	2
ϱ_{calc}/Mg · m^{-3}	1.931 (3) (T = 297 K)	1.823 (3) (T = 297 K)	1.550(1) (T = 298 K)
ϱ_{pykn}/Mg · m^{-3}	1.92 (T = 295 K)	1.81 (T = 294 K)	1.48 (T = 295 K)
Point positions:	all atoms in 4a:	all atoms in 4a:	all atoms in 2a:
	x, y, z; $\frac{1}{2}-x, \bar{y}, \frac{1}{2}+z$;	see left column	x, y, z; $\bar{x}, \frac{1}{2}+y, \bar{z}$
	$\frac{1}{2}+x, \frac{1}{2}-y, \bar{z}$; $\bar{x}, \frac{1}{2}+y, \frac{1}{2}-z$		

Nuclear Quadrupole Resonance

The NQR spectra of the title compounds (Table 1) were measured with a superregenerative oscillator type spectrometer, lock in technique, time constant 10 s. Most NQR spectra have been studied as functions of temperature to look for solid ↔ solid phase transitions. The wanted temperatures at the sample site were generated by liquid nitrogen (77 K), by a flow and temperature regulated stream of nitrogen gas (100–200 K), by a cryostat with methanol as cooling liquid (200–300 K), and by a thermostat with oil as medium ($T > 300$ K). The temperature of the samples was determined by thermocouples (Cu/Constantan) to ± 0.3 K, and the frequencies were measured by counting to ± 5 kHz. In all measurements of bromine NQR, for both isotopes, ^{79}Br and ^{81}Br, the NQR frequencies have been observed at selected temperatures to find unique assignment. This is a fairly simple and safe procedure since the ratio of the nuclear quadrupole moments $Q(^{79}\text{Br})/Q(^{81}\text{Br})$ is well known and the ratio of the frequencies is equal to that of the nuclear quadrupole moments. In the following we give only the ^{79}Br NQR frequencies in figures and tables. We mention that several amino acid hydrohalides and dipeptide hydrohalides not listed in Table 1 have been synthesized and investigated by NQR without success, probably because of improper crystallization.

Crystal Structure Determination

The crystal structures of L-histidine dihydrobromide, L-His · 2 HBr, of L-cysteine hydrobromide monohydrate, L-Cys · HBr · H_2O and of glycyl-L-leucine hydroiodide monohydrate, Gly-L-Leu · HI · H_2O, were determined with a 4-circle X-ray diffractometer using small single crystals grown from aqueous solution of the respective compound. The intensities collected were corrected for absorption and Lorentz-polarisation factor. The structures were solved by direct methods and the hydrogen atoms found from Fourier synthesis [6]. The structures were refined by least squares procedures [7]. In Table 2 the experimental conditions for the crystal structure determinations are given, including crystallographic data of the title compounds. The final structure amplitudes, F_o and F_c, can be found in [5].

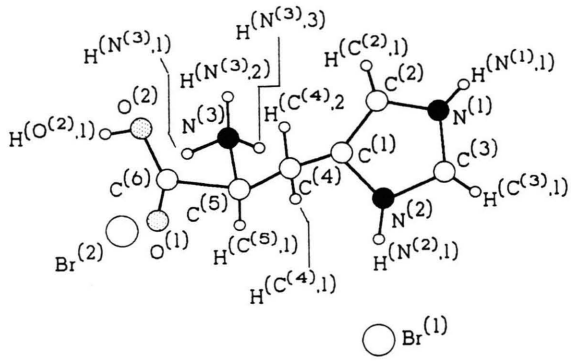

Fig. 1. Formula unit of L-histidine dihydrobromide. The sketch is according to the position of the formula unit in the unit cell.

Table 3. Inter- and intramolecular bond distances (in pm) and bond angles (in degree) of L-histidine dihydrobromide. For the numbering, see Fig. 1 and Table A.1.

Connection (distance)	d/pm	Connection (angle)	Angle/°
$C^{(1)}-C^{(2)}$	135.0(5)	$C^{(1)}-C^{(2)}-N^{(1)}$	106.7(4)
$C^{(2)}-N^{(1)}$	138.3(5)	$C^{(2)}-N^{(1)}-C^{(3)}$	108.7(4)
$N^{(1)}-C^{(3)}$	132.0(5)	$N^{(1)}-C^{(3)}-N^{(2)}$	108.7(4)
$C^{(3)}-N^{(2)}$	131.3(5)	$C^{(3)}-N^{(2)}-C^{(1)}$	109.3(4)
$N^{(2)}-C^{(1)}$	137.7(5)	$N^{(2)}-C^{(1)}-C^{(2)}$	106.5(3)
$C^{(1)}-C^{(4)}$	149.0(5)	$N^{(2)}-C^{(1)}-C^{(4)}$	124.3(4)
$C^{(4)}-C^{(5)}$	154.7(6)	$C^{(2)}-C^{(1)}-C^{(4)}$	129.2(4)
$C^{(5)}-N^{(3)}$	149.3(5)	$C^{(1)}-C^{(4)}-C^{(5)}$	113.2(3)
$C^{(5)}-C^{(6)}$	152.4(5)	$C^{(4)}-C^{(5)}-C^{(6)}$	109.5(3)
$C^{(6)}-O^{(1)}$	119.5(4)	$C^{(4)}-C^{(5)}-N^{(3)}$	110.9(3)
$C^{(6)}-O^{(2)}$	131.8(5)	$N^{(3)}-C^{(5)}-C^{(6)}$	109.3(3)
$Br^{(1)}\cdots N^{(2)}$	326.7	$C^{(5)}-C^{(6)}-O^{(1)}$	123.4(4)
$Br^{(1)}\cdots N^{(3)'}$	327.5	$C^{(5)}-C^{(6)}-O^{(2)}$	110.9(4)
$Br^{(1)}\cdots O^{(2)'}$	310.2	$O^{(1)}-C^{(6)}-O^{(2)}$	125.7(3)
$Br^{(2)}\cdots N^{(3)}$	328.3	$C^{(6)}-O^{(2)}-H^{(O^{(2)},1)}$	106.6(34)
$Br^{(2)}\cdots N^{(1)}$	326.0		

Table 4. Hydrogen bond lengths (in pm) and bond angles (in degrees) of L-histidine dihydrobromide. A = Hydrogen acceptor; D = Hydrogen donor.

Connection	d(A···D) [pm]	d(H···A) [pm]	d(H–D) [pm]	∢(A···H–D) [°]
$Br^{(1)\,I}\cdots H(N^{(2)},1)$	326.7	238.1	93.0(38)	159.1
$Br^{(1)\,II}\cdots H(N^{(3)},3)$	327.5	234.8	95.4(42)	163.8
$Br^{(1)\,III}\cdots H(O^{(2)},1)$	310.2	226.6	86.5(43)	162.7
$Br^{(2)\,IV}\cdots H(N^{(1)},1)$	326.0	219.8	108.9(47)	164.3
$Br^{(2)\,V}\cdots H(N^{(3)},1)$	328.3	236.7	101.3(40)	149.4
$O^{(1)\,VI}\cdots H(N^{(3)},2)$	289.4	201.0	92.7(46)	158.7

Point positions: $Br^{(1)\,I}$: x, y, z; $Br^{(1)\,II}$: $\frac{1}{2}-x, 1-y, \frac{1}{2}-z$: $Br^{(1)\,III}$: $1-x, \frac{1}{2}+y, \frac{1}{2}-z$; $Br^{(2)\,IV}$: $-\frac{1}{2}+x, \frac{3}{2}-y, 1-z$; $Br^{(2)\,V}$: x, y, z; $O^{(1)\,VI}$: $1-x, \frac{1}{2}+y, \frac{1}{2}-z$.

Results

Crystal Structures of L-His · 2 HBr, L-Cys · HBr · H_2O, and Gly-L-Leu · HI · H_2O

The metric of the unit cells of the title compounds, R-values, experimental conditions, etc. are given in Table 2. For clearness we show the relative coordinates of the crystal structures as well as the thermal parameters in tables of the Appendix A. The positional and thermal parameters of L-His · 2 HBr are given in Table A.1. Table A.2 lists these data for L-Cys · HBr · H_2O, and for Gly-L-Leu · HI · H_2O the corresponding data are given in Table A.3.

L-Histidine dihydrobromide, L-His · 2 HBr

The compound L-His · 2 HBr is composed of a double protonated anion $(\text{L-His} \cdot H_2)^{2\oplus}$ and two $Br^{\ominus}$. The positive charges should be located at the NH_3 group and at the imidazole ring, respectively. In the latter one both nitrogen atoms are protonated. In Fig. 1 we show the geometry of a formula unit of L-His · 2 HBr, as it is found in the unit cell. The crystal lattice of L-His · 2 HBr is governed by hydrogen bonds, connecting anions and cations within the unit cell to a three-dimensional network. In Fig. 2 the projection of the orthorhombic unit cell of L-His · 2 HBr along the c-axis onto the (ab)-plane is shown. The hydrogen bonds are marked by dashed lines.

For the discussion of the bond scheme in L-His · 2 HBr let us have a look on the intra- and intermolecular distances listed in Table 3. The hydrogen bond distances and bond angles are given in Table 4. Along the a-axis chains of L-His ions and bromine ions are formed in which the ions are connected by hydrogen bonds $O-H\cdots Br^{\ominus}$ and $N-H\cdots Br^{\ominus}$. In the directions of the b- and c-axis a hydrogen bond net is formed by bonds $N-H\cdots O$ and $N-H\cdots Br^{\ominus}$. Each ammonium group forms one hydrogen bond to the atom $Br^{(1)}$, one to $Br^{(2)}$, and one to the carboxyl oxygen of the acid group COOH. The hydrogen atom of the COOH-group forms also a hydrogen bond to one of the bromines and finally from both NH groups within the protonated imidazole ring a hydrogen bond is directed to a bromine (see Table 4). As a result, one of the bromines accepts two hydrogen bonds $N-H\cdots Br^{\ominus}$; the other bromine accepts an additional bond $O-H\cdots Br^{\ominus}$. Comparison shows that L-His · 2 HBr is isostructural with L-His · 2 HCl, the structure of which is reported in [8, 9].

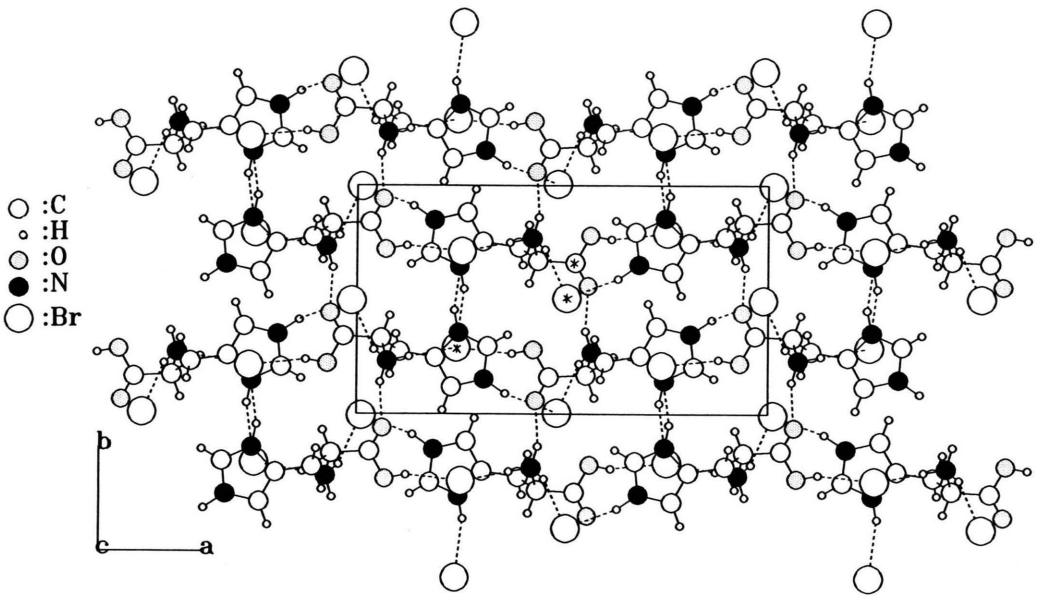

Fig. 2. Projection of the unit cell of L-histidine dihydrobromide along the *c*-axis onto the plane (*ab*). The hydrogen bonds are marked by dashed lines. The stared unit is the one for which the coordinates are given in Table A.1.

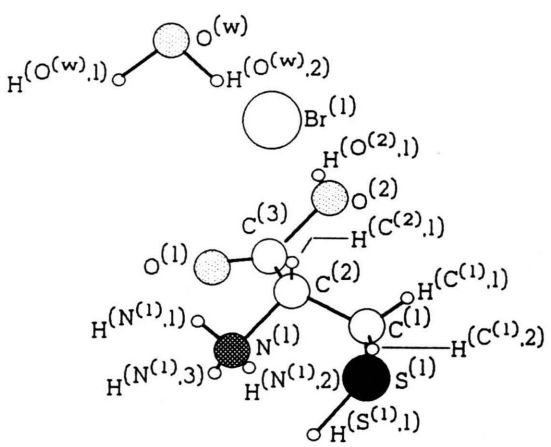

Fig. 3. Formula unit of L-cysteine hydrobromide monohydrate. The sketch corresponds to the positions of the formula unit in the unit cell.

Looking on intramolecular bond distances and angles of L-His compounds, in which both nitrogens of the imidazole ring are protonated and for which the crystal structure is reported, the data given in Table 3 agree well with the distances and angles reported for L-His · HCl · H_2O [10–12], Cu(L-His · NO_3 · $H_2O)_2$ [13], DL-His · HCl · 2 H_2O [14], L-His · 2 HCl [8, 9], L-His · L-Asp · H_2O [15]. Bond angles and bond lengths of the imidazole ring in neutral histidine differ somewhat from the protonated ring as found for orthorhombic L-His [16, 17], monoclinic L-His [18] and DL-His [19]. About the intramolecular distances within the amino acid group (Table 3) we can say that they are found in a range observed for a large number of amino acid derivatives [20, 21].

L-Cysteine hydrobromide monohydrate, L-Cys · HBr · H_2O

The formula unit of L-Cys · HBr · H_2O is sketched in Fig. 3 with respect to the unit cell of the title compound. The coordinates of the atoms and the thermal parameters are listed in Table A.2; in Fig. 4 we show the projection of the unit cell along [001] onto the plane (*ab*). Again the hydrogen bonds are marked by dashed lines. In Table 5 the intra- and intermolecular distances and angles are given and in Table 6 the distances and angles determining the hydrogen bond scheme.

The bond distances and bond angles within the L-cysteine molecule of L-Cys · HBr · H_2O are comparable with the ones observed for other cysteine compounds such as L-Cys · HCl · H_2O [22, 23], orthorhombic L-Cys [24, 25], and monoclinic L-Cys [26]. Bond lengths and bond angles of the amino acid group are within the region found for many amino acid and peptide compounds [20, 21].

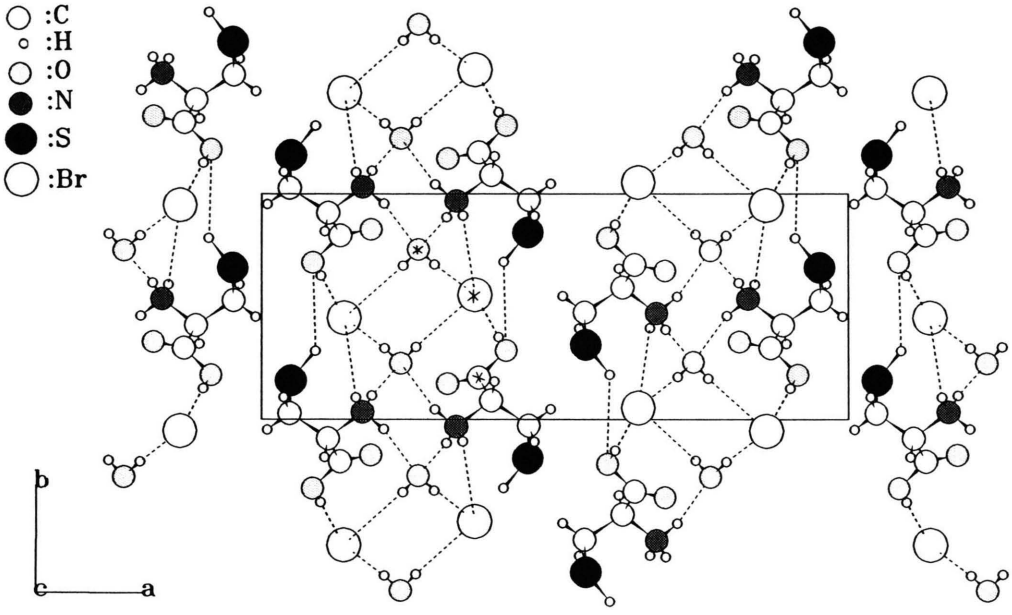

Fig. 4. Projection of the unit cell of L-cysteine hydrobromide monohydrate along [001] onto the plane (*a b*). The stared unit is the one for which the coordinates are given in Table A.2.

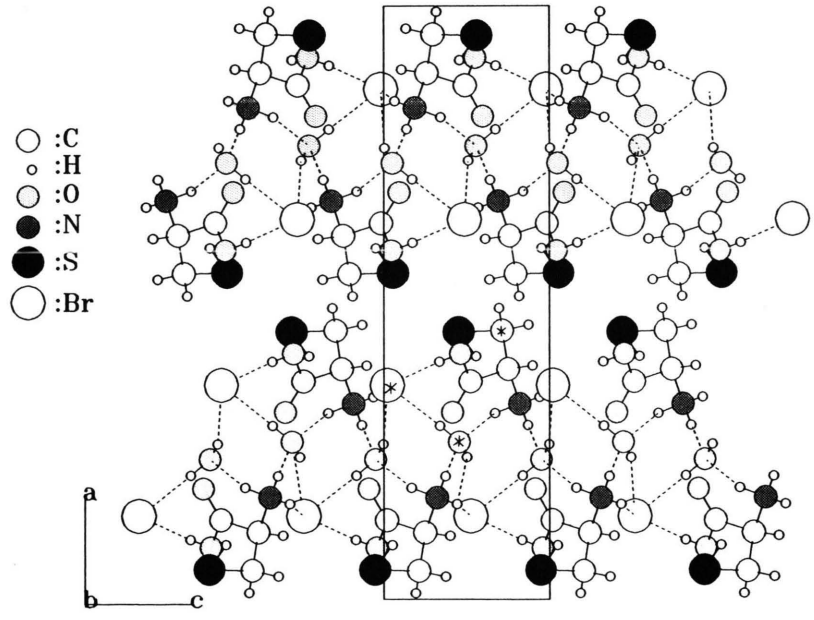

Fig. 5. Projection of the unit cell of L-cysteine hydrobromide monohydrate along [010] onto the plane (*a c*). The coordinates of the stared unit are given in Table A.2.

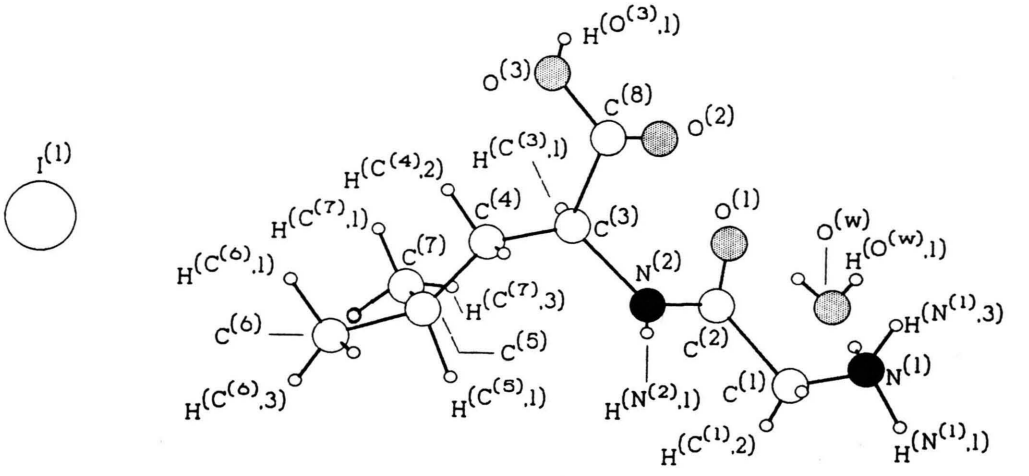

Fig. 6. Formula unit of glycyl-L-leucine hydroiodide monohydrate. The sketch corresponds to the position of the formula unit in the unit cell.

Table 5. Intra- and intermolecular bond distances (in pm) and angles (in degree) of L-cysteine hydrobromide monohydrate. For the numbering of the atoms see Fig. 3 and Table A.2.

Connection (distance)	d/pm	Connection (angle)	Angle/°
$H(S^{(1)},1)-S^{(1)}$	139.9(25)	$H(S^{(1)},1)-S^{(1)}-C^{(1)}$	95.9(13)
$S^{(1)}-C^{(1)}$	180.2(3)	$S^{(1)}-C^{(1)}-C^{(2)}$	114.4(2)
$C^{(1)}-C^{(2)}$	152.8(3)	$C^{(1)}-C^{(2)}-C^{(3)}$	112.3(2)
$C^{(2)}-C^{(3)}$	152.0(3)	$C^{(1)}-C^{(2)}-N^{(1)}$	111.2(2)
$C^{(2)}-N^{(1)}$	148.4(3)	$N^{(1)}-C^{(2)}-C^{(3)}$	107.4(2)
$C^{(3)}-O^{(1)}$	119.5(3)	$C^{(2)}-C^{(3)}-O^{(1)}$	123.4(2)
$C^{(3)}-O^{(2)}$	131.4(2)	$C^{(2)}-C^{(3)}-O^{(2)}$	111.0(2)
$O^{(w)}\cdots N^{(1)}$	286.2	$O^{(1)}-C^{(3)}-O^{(2)}$	125.5(2)
$O^{(w)}\cdots N^{(1)'}$	286.2	$C^{(3)}-O^{(2)}-H(O^{(2)},1)$	110.0(19)
$Br^{(1)}\cdots O^{(w)}$	336.3	$H(O^{(w)},1)-O^{(w)}-H(O^{(w)},2)$	
$Br^{(1)}\cdots O^{(w)}$	335.1		102.2(26)

Table 6. Hydrogen bond lengths (in pm) and bond angles (in degrees) of L-cysteine hydrobromide monohydrate; A = Hydrogen acceptor, D = Hydrogen donor.

Connection	d(A···D) [pm]	d(A···H) [pm]	d(D–H) [pm]	∢(D–H···A) [°]
$Br^{(1)I}\cdots H(O^{(2)},1)$	320.5	234.1	86.7(29)	173.4
$Br^{(1)II}\cdots H(N^{(1)},2)$	335.9	269.5	84.7(31)	136.4
$Br^{(1)III}\cdots H(O^{(w)},1)$	335.1	260.1	77.7(26)	162.6
$Br^{(1)IV}\cdots H(O^{(w)},2)$	336.3	239.6	97.1(30)	173.9
$O^{(w)V}\cdots H(N^{(1)},1)$	286.2	194.7	93.5(28)	165.4
$O^{(w)VI}\cdots H(N^{(1)},3)$	286.2	184.3	104.4(32)	164.1
$O^{(2)VII}\cdots H(S^{(1)},1)$	398.5	298.6	139.3(25)	127.2
$Br^{(1)VIII}\cdots H(S^{(1)},1)$	416.4	296.3	139.3(25)	143.4

Point positions: $Br^{(1)I}$: x, y, z; $Br^{(1)II}$: $x, y-1, z+1$; $Br^{(1)III}$: $\frac{1}{2}-x, 1-y, \frac{1}{2}+z$; $Br^{(1)IV}$: x, y, z; $O^{(w)V}$: $\frac{1}{2}-x, 1+y, \frac{1}{2}+z$; $O^{(w)VI}$: $x, y-1, z$; $O^{(2)VII}$: $x, y-1, z$; $Br^{(1)VIII}$: $x, y-1, z+1$.

In the crystal lattice of L-Cys · HBr · H_2O the bromine ions, the positively charged L-Cys ions, and the water molecules are connected by hydrogen bonds, forming twodimensional layers. These layers are clearly seem in the projection of the unit cell along [010] onto the plane (ac), see Figure 5. They are parallel to the bc-plane, centered at $x=0.25$ and $x=0.75$ (compare Figs. 4 and 5). Van der Waals interaction via the molecule part $C^{(1)}H_2$–SH holds the layers together. $Br^{\ominus}$ is surrounded by three hydrogen bonds O–H ··· $Br^{\ominus}$ and one hydrogen bond N–H ··· $Br^{\ominus}$. The bonds O–H ··· $Br^{\ominus}$ are provided by two different H_2O molecules and by the carboxyl group of the L-Cys molecule. The ammonium group of the L-Cys molecule forms a hydrogen bond N–H ··· $Br^{\ominus}$ and two bonds N–H ··· O to two different H_2O molecules. The hydrogen bond network (see also Table 6) corresponds to the one found for L-Cys · HCl · H_2O [23]. The carboxyl oxygen $O^{(1)}$ is a possible hydrogen acceptor but it is not incorporated in the hydrogen bond system.

However, there are possibilities of the thiol group to form hydrogen bonds. Paul [27] has shown that for formation of an S–H hydrogen bond several criteria must be fulfilled. The distance between the sulfur atom and the proton acceptor atom A should be smaller than $d = 235$ pm $+ r_{vdw}$(A) (r_{vdw} = van der Waals radius) and the angle $C^{(1)}-S^{(1)}\cdots$A should be 90° (±20–30°). From difference Fourier synthesis we found a hydrogen position for the thiol group which has a short distance to two acceptor atoms, $Br^{(1)}$ and $O^{(2)}$ (see Table 5). For L-Cys · HCl · H_2O Ramachandra [23]

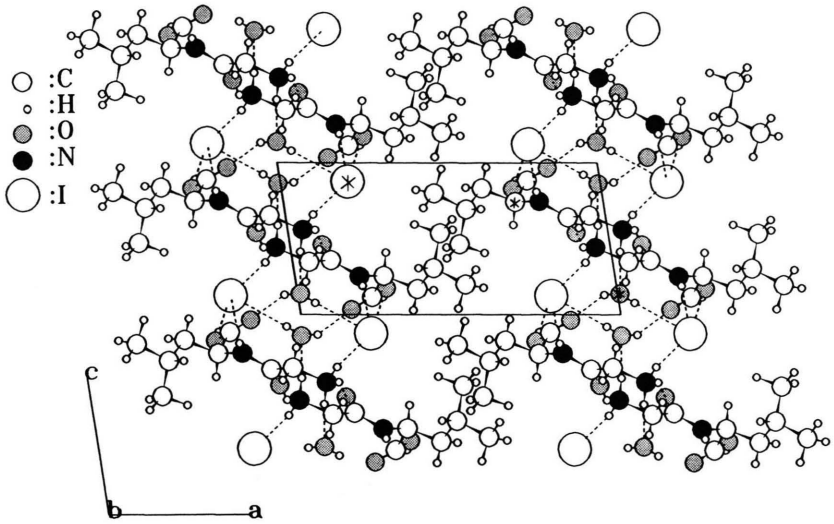

Fig. 7. Projection of the unit cell fo glycyl-L-leucine hydroiodide monohydrate along the twofold axis onto the plane (*ac*). The unit marked by *) is the one for which the coordinates are given in Table A.3.

Table 7. Intra- and intermolecular bond distances (in pm) and bond angles (in degree) of glycyl-L-leucine hydroiodide monohydrate, Gly-L-Leu · HI · H_2O. For the numbering of the atoms see Fig. 6 and Table A.3.

Connection (distance)	*d*/pm	Connection (angle)	Angle/°
$N^{(1)}-C^{(1)}$	148.0(4)	$N^{(1)}-C^{(1)}-C^{(2)}$	110.4(2)
$C^{(1)}-C^{(2)}$	151.5(3)	$C^{(1)}-C^{(2)}-N^{(2)}$	114.9(2)
$C^{(2)}-O^{(1)}$	122.2(3)	$C^{(1)}-C^{(2)}-O^{(1)}$	121.8(2)
$C^{(2)}-N^{(2)}$	132.1(3)	$O^{(1)}-C^{(2)}-N^{(2)}$	123.3(2)
$N^{(2)}-C^{(3)}$	144.9(3)	$C^{(2)}-N^{(2)}-C^{(3)}$	121.9(2)
$C^{(3)}-C^{(4)}$	153.1(4)	$N^{(2)}-C^{(3)}-C^{(4)}$	110.9(2)
$C^{(4)}-C^{(5)}$	152.7(4)	$C^{(3)}-C^{(4)}-C^{(5)}$	114.5(3)
$C^{(5)}-C^{(6)}$	150.3(5)	$C^{(4)}-C^{(5)}-C^{(6)}$	109.1(3)
$C^{(5)}-C^{(7)}$	147.2(5)	$C^{(4)}-C^{(5)}-C^{(7)}$	113.4(3)
$C^{(3)}-C^{(8)}$	152.4(3)	$C^{(6)}-C^{(5)}-C^{(7)}$	109.5(4)
$C^{(8)}-O^{(2)}$	119.4(3)	$N^{(2)}-C^{(3)}-C^{(8)}$	110.5(2)
$C^{(8)}-O^{(3)}$	132.2(3)	$C^{(4)}-C^{(3)}-C^{(8)}$	108.9(2)
$I^{(1)}\cdots N^{(1)}$	365.2	$C^{(3)}-C^{(8)}-O^{(2)}$	126.1(2)
$I^{(1)}\cdots N^{(2)}$	372.7	$C^{(3)}-C^{(5)}-O^{(3)}$	109.7(2)
$I^{(1)}\cdots O^{(3)}$	348.0	$O^{(2)}-C^{(8)}-O^{(3)}$	124.1(2)
$I^{(1)}\cdots O^{(w)}$	354.8	$H^{(1)}(O^{(w)})-O^{(w)}-H^{(2)}(O^{(w)})$	
$O^{(1)}\cdots N^{(1)}$	279.3		103.3(30)
$O^{(2)}\cdots O^{(w)}$	290.4	$H^{(1)}(O^{(3)})-O^{(3)}-C^{(8)}$	
$N^{(1)}\cdots O^{(w)}$	278.5		116.7(25)

Table 8. Hydrogen bond lengths (in pm) and bond angles (in dregrees) of glycyl-L-leucine hydroiodide monohydrate, A = Hydrogen acceptor, D = Hydrogen donor.

Connection	*d*(A···D) [pm]	*d*(A···H) [pm]	*d*(D–H) [pm]	∢(D–H···A) [°]
$I^{I}\cdots H^{(3)}(N^{(1)})$	365.3	271.2	95.2(29)	169.6
$I^{II}\cdots H^{(1)}(O^{(3)})$	348.0	273.0	75.0(30)	174.6
$I^{III}\cdots H^{(1)}(N^{(2)})$	372.7	302.7	70.4(28)	173.1
$I^{IV}\cdots H^{(1)}(O^{(w)})$	354.8	273.8	82.4(31)	167.8
$O^{(1)V}\cdots H^{(1)}(N^{(1)})$	279.3	186.2	99.9(29)	153.7
$O^{(w)VI}\cdots H^{(2)}(N^{(1)})$	278.5	180.2	98.9(34)	172.3
$O^{(2)VII}\cdots H^{(2)}(O^{(w)})$	290.4	213.5	79.1(29)	154.1

Point positions: I^{I}: $x+1, y, z$; I^{II}: $-x+1, y+\frac{1}{2}, -z+2$; I^{III}: $-x+1, y-\frac{1}{2}, -z+2$; I^{IV}: $x+1, y, z-1$; $O^{(1)V}$: $-x+1, y-\frac{1}{2}, z$; $O^{(w)VI}$: x, y, z; $O^{(2)VII}$: $x, y, z-1$.

discusses a hydrogen bond S–H ··· $Cl^{\ominus}$, and in the title compound a bond S–H ··· $Br^{\ominus}$ may exist. Then, however, it would be necessary to replace one of the four hydrogen bonds X–H ··· $Br^{\ominus}$ already assumed above in the hydrogen bonding system for L-Cys · HBr · H_2O. Also the angle $C^{(1)}-S^{(1)}\cdots Br^{(1)}$ is 151.2° (in L-Cys · HCl · H_2O 151°), too large for a hydrogen bond [27]. In L-Cys · HBr · H_2O an S–H ··· O bond is the only chance to incorporate the thiol group into the hydrogen bond system.

Glycyl-L-leucine hydroiodide monohydrate, Gly-L-Leu · HI · H_2O

The title compound Gly-L-Leu · HI · H_2O crystallizes monoclinic, $P2_1$, $Z=2$ (see Table 2). In Fig. 6 the formula unit is sketched and in Fig. 7 we show the projection of the unit cell along the two-fold axis [010] onto the plane (*ac*). In Table A.3 the positional coordinates and thermal parameters are given, and in Table 7 we list the prominent intra- and intermolecular bond distances and bond angles. The characteristic hydrogen bonds are given in Table 8.

Table 9. Conformational angles of His · 2 HBr, Cys · HBr · H_2O, and Gly-L-Leu · HI · H_2O and similar compounds. The definition of the torsion angles is according to that of the IUPAC-IUB Commission on Biochemical Nomenclature [76].

Substance	ψ	ω	φ	ψ^1	ψ^2	χ^1	χ^{21}	χ^{22}	Ref.
L-His · 2 HCl				153.9	−27.1	−53	−75		[9]
L-His · 2 HBr				153.8	−26.8	−53.4	−76.0		*
L-Cys · HCl · H_2O				−5.9	173.4	64.9			[23]
L-Cys · HBr · H_2O				−6.5	173.5	69.2			*
Gly-L-Ala · HBr · H_2O	168.4	179.0	−126.0	−11.9	169.2				[72]
Gly-L-Ala · HI · H_2O	168.1	177.9	−126.3	−12.9	167.8				[72]
Gly-L-Leu	171.6	168.7	−64.9	−30.2	151.9	−175.8	62.9	−173.0	[28]
Gly-L-Leu · HI · H_2O	−171.4	−176.8	−72.8	−25.1	155.4	−62.6	178.2	−59.5	*

* This paper.

Gly-L-Leu · HI · H_2O is an ambiphilic system with hydrophobic (lipophilic) interactions in the one part of the salt and hydrophilic (lipophobic) interactions in the other one. The isobutyl group of the leucine unit is strongly hydrophobic; the peptide backbone, with the amido-, ammonium-, and acid group, including H_2O and the iodine ion, is strongly hydrophilic. This shows up in the crystal structure. Parallel to the bc-plane a double layer lattice is formed (see Figure 7). At $x=\frac{1}{2}$ the isobutyl groups of two molecules interact, forming a layer, and at $x=0$ the peptide rests, including $I^{\ominus}$ and H_2O, form a second layer. In total, a sandwich with the charged part and the hydrogen bonding groups at the inside, the isobutyl groups as the covers, appears. The hydrogen bonds connect the layer at $x=0$ to a twodimensional net, and the van der Waals interactions hold the layers together. This layer structure reminds of similar structures of Gly-L-Leu [28], L-Leu · HBr [29], L-Leu · HI [30], D-Leu-Gly · HBr [31], and D-Ile · HBr · H_2O [32].

The hydrogen bond system involves seven bonds: one from the NH group as donor, three from the NH_3 group, two from the water molecule, and one from the acid group COOH. Four hydrogen bonds are accepted by $I^{\ominus}$, two of the type N–H ··· $I^{\ominus}$ and two of the type O–H ··· $I^{\ominus}$. The bond distance between the OH group of COOH and $I^{\ominus}$ is rather short. The second O–H···$I^{\ominus}$ bond is due to the water molecule. The hydrogen bonds N–H ··· $I^{\ominus}$ are donated by the amide proton and one of the ammonium protons, respectively. The remaining two protons of the ammonium groups form an N–H ··· O bond with the carboxyl oxygen of the peptide bond and with the oxygen of the water molecule. Finally, there is an O–H ··· O bond between the second proton of the water molecule and the carboxyl oxygen of the acid group.

Conformation Analysis

The conformation of an amino acid or peptide is described by a set of torsion angles. In Table 9 there are given all the torsion angles of the title compounds for which the crystal structure is reported here. For comparison, data for structurally related compounds are listed, too. The definition of the torsion angles is according to the IUPAC-IUB convention on biochemical nomenclature [76]. For amino acids one needs only the torsion angles ψ^1 and ψ^2 and angles χ^i ($i=1, 2, \ldots$) to describe the side chain of the amino acid. $\chi^{1,2}$ should be near 0° or 180° (±20–30°) [77] and χ^1 of a single side chain bond should be around −60°, 60°, and 180° [78]. For many cysteine compounds χ^1 is in the range $55 \leq \chi^1/° \leq 75$ [78]. From Table 9 one finds that this is valid for L-Cys · HBr · H_2O. For the side chain of the histidine molecule a second side chain torsion angle χ^{21} must be considered. χ^{21} should be in the range ±90° (±20–30°) [15]. If $\chi^1 \approx -60°$ or 180°, then the imidazole ring has the so-called "open" conformation. If $\chi^1 \approx +60°$, then the histidine is in the "closed" form [15]. In L-His · 2 HBr the imidazole ring is in the sterically preferred "open" conformation (Table 9). The imidazole ring with the atoms $C^{(1)}$, $C^{(2)}$, $N^{(1)}$, $C^{(3)}$, and $N^{(2)}$ is nearly planar; the deviations from planarity are small. (The plane equation is: $223.43\,x - 45.36\,y + 712.99\,z = 151.68$ pm). In peptides there exist torsion angles φ, ψ, and ω. The torsion angle ω should be near 0° or 180°; in the sterically preferred trans-conformation of a peptide it is near 180°, so for Gly-L-Leu · HI · H_2O, see Table 9. For the torsion angles φ and ψ there exist energetically preferred special combinations according to the side chain. In a φ, ψ-conformation map the energetically preferred regions are described [76]. The φ, $\psi^{1,2}$-combination of Gly-L-Leu · HI · H_2O is in one of these

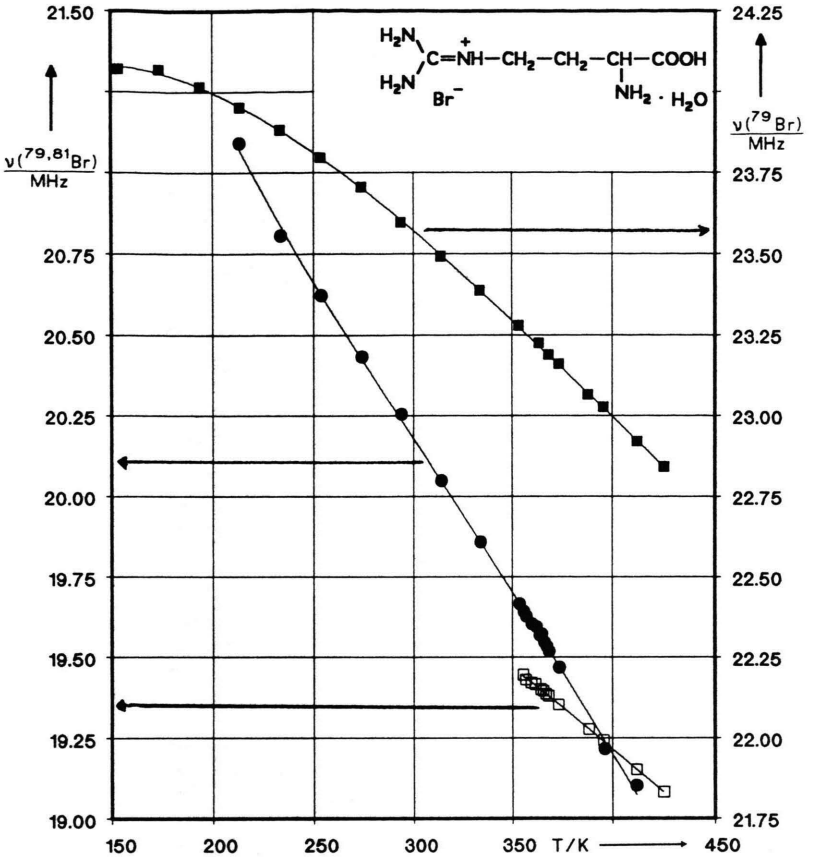

Fig. 8. ^{79}Br NQR spectrum of L-arginine hydrobromide monohydrate as a function of temperature. For the parameterization of the curves see Table A.4. $\nu_1(^{79}Br)$: ●; $\nu_2(^{79}Br)$: ■; $\nu_2(^{81}Br)$: □.

regions. The change of sign of the glycyl-peptides for ψ and ω in Table 9 is due to the glycyl residue (no asymmetric C-atom), for which positive and negative values are possible. In case of the side chain of a leucyl residue there are only two combinations of χ^1 and χ^{21} energetically preferred (180°, 60° and −60°, 180°) [79]. Peptides select the second possibility, so Gly-L-Leu · HI · H_2O. In this conformation $C^{(5)}$ is in gauche position to the carbon atom of the acid group and to the nitrogen atom of the peptide bond.

Table 10. Hydrogen bond distances A ··· H–D (A = acceptor atom, D = donor atom) [35] in L-arginine hydrobromide monohydrate.

Connection A ··· D	d(A ··· D)/pm
$Br^{(1)} \cdots N^{(1)}$ (NH_3)	335.0
$Br^{(1)} \cdots N^{(2)}$ (Guanidyl)	342.0
$Br^{(1)} \cdots N^{(3)}$ (Guanidyl)	335.8
$Br^{(1)} \cdots O$ (H_2O)	337.1
$Br^{(2)} \cdots N^{(1)}$ (NH_3)	337.4
$Br^{(2)} \cdots N^{(2)}$ (Guanidyl)	340.9
$Br^{(2)} \cdots N^{(3)}$ (Guanidyl)	350.3
$Br^{(2)} \cdots O$ (H_2O)	322.9

Halogen NQR Spectra of the Title Compounds

^{79,81}Br NQR

L-Arginine hydrobromide monohydrate, L-Arg · HBr · H_2O

The crystal structure of L-Arg · HBr · H_2O is known, $P2_1$, $Z=4$ [33–36]. In the frequency range $8 \leq \nu/\text{MHz} \leq 32$ four resonance signals are observed, which can be assigned to the two crystallographically inequivalent bromine positions of ^{79,81}Br. $\nu_{1,2}(^{79}Br)/\nu_{1,2}(^{81}Br) = 1.1968$ was found. In Fig. 8 the ^{79}Br NQR frequencies are plotted in their dependence on temperature in the range $154 \leq T/\text{K} \leq 425$. The curves are smooth functions of T, in agreement with the results of the differential thermal analysis, DTA, in which no sign for a phase transition was observed within $77 \leq T/\text{K} \leq 448$. The signal to noise ratio, S/N, of the

Table 11. The ^{79}Br- and ^{127}I-NQR-frequencies of the compounds investigated at selected tmperatures (preferable at $T = 77$ K and $T = 293$ K) and their signal to noise ratio (S/N).

Substance	NQR-signal	T/K	ν/MHz	S/N	T/K	ν/MHz	S/N
L-Arg · HBr · H_2O	$\nu_1(^{79}Br)$	213	21.093	3	294	20.257	8
	$\nu_2(^{79}Br)$	153	24.068	3	294	23.596	15
L-Cys · HBr · H_2O	$\nu(^{79}Br)$	77	14.238	7	288	14.914	24
L-Cys-S-S-L-Cys · 2 HBr	$\nu(^{79}Br)$	77	23.289	5	289	21.680	11
Ethanolamine · HBr	$\nu(^{79}Br)$	77	20.033	15	288	19.424	75
L-Glu · HBr	$\nu(^{79}Br)$	77	12.770	4	288	12.292	7
L-His · HBr	$\nu(^{79}Br)$	77	21.412	5	288	20.053	6
L-His · 2 HBr	$\nu_1(^{79}Br)$	77	18.496	20	288	17.689	24
	$\nu_2(^{79}Br)$	77	28.382	10	288	27.015	13
L-Ile · HBr · H_2O	$\nu(^{79}Br)$	273	15.971	2	290	16.019	6
Sar · HBr	$\nu(^{79}Br)$	77	18.343	80	293	17.786	30
Sar_2 · HBr	$\nu_1(^{79}Br)$	77	17.485	3	294	15.652	5
	$\nu_2(^{79}Br)$	233	17.619	2	294	16.700	4
L-Val · HBr · H_2O	$\nu(^{79}Br)$	273	16.602	2	290	16.598	6
Ethanolamine · HI [a]	$\nu_1(^{127}I)$	77	17.778	90	287	15.889	120
	$\nu_2(^{127}I)$	77	22.073	80	287	19.121	100
Sar · HI (from solution) [b]	$\nu_1^I(^{127}I)$	77	23.779	4	293	20.620	10
Phase I	$\nu_2^I(^{127}I)$	77	40.293	10	293	35.792	5
(from melting) [b]	$\nu_1^{II}(^{127}I)$	120	24.638	5	293	24.363	15
Phase II	$\nu_2^{II}(^{127}I)$	253	27.060	2	293	26.620	10
Gly_2 · HI	$\nu_1(^{127}I)$	163	19.762	3	288	18.692	10
	$\nu_2(^{127}I)$	174	21.228	3	288	20.638	10
	$\nu_3(^{127}I)$	77	22.379	4	288	21.921	10
	$\nu_4(^{127}I)$	77	25.086	4	288	25.727	10
Sar_2 · HI [c]	$\nu_1(^{127}I)$	77	14.691	10	294	13.843	5
	$\nu_2(^{127}I)$	77	18.983	10	294	16.535	5
Gly-L-Leu · HI · H_2O [d]	$\nu_1(^{127}I)$	77	23.375	10	287	22.854	8
	$\nu_2(^{127}I)$	77	27.534	15	287	25.449	10

[a] $e\Phi_{zz}Qh^{-1}(^{127}I)$: 80.033 MHz, $\eta(^{127}I)$: 0.7466 ($T = 77$ K); $e\Phi_{zz}Qh^{-1}(^{127}I)$: 69.707 MHz, $\eta(^{127}I)$: 0.7805 ($T = 287$ K);
[b] $e\Phi_{zz}Qh^{-1}(^{127}I)^I$: 138.022 MHz, $\eta(^{127}I)$: 0.3832 ($T = 77$ K); $e\Phi_{zz}Qh^{-1}(^{127}I)^I$: 122.288 MHz, $\eta(^{127}I)^I$: 0.3552 ($T = 290$ K); $e\Phi_{zz}Qh^{-1}(^{127}I)^{II}$: 100.347 MHz, $\eta(^{127}I)^{II}$: 0.8806 ($T = 253$ K); $e\Phi_{zz}Qh^{-1}(^{127}I)^{II}$: 99.033 MHz, $\eta(^{127}I)^{II}$: 0.8921 ($T = 290$ K).
[c] $e\Phi_{zz}Qh^{-1}(^{127}I)$: 68.291 MHz, $\eta(^{127}I)$: 0.7013 ($T = 77$ K); $e\Phi_{zz}Qh^{-1}(^{127}I)$: 60.613 MHz, $\eta(^{127}I)$: 0.7848 ($T = 290$ K).
[d] $e\Phi_{zz}Qh^{-1}(^{127}I)$: 100.833 MHz, $\eta(^{127}I)$: 0.8061 ($T = 77$ K); $e\Phi_{zz}Qh^{-1}(^{127}I)$: 94.036 MHz, $\eta(^{127}I)$: 0.8733 ($T = 290$ K).

lower frequency signal $\nu_1(^{79}Br)$ decreases from 8 at 350 K to 3 at 213 K; it was unobservable at lower temperatures. The higher frequency $\nu_2(^{79}Br)$ signal shows S/N = 20 at 374 K; S/N decreases to 3 at 154 K and the signal cannot be followed up at lower temperatures. The two bromine atoms have different hydrogen bond distances. There is one hydrogen bond $N-H\cdots Br^{\ominus}$ provided by the amino group and two bonds $N-H\cdots Br^{\ominus}$ by the guanidyl group. A fourth hydrogen bond, $O-H\cdots Br^{\ominus}$, is due to the water molecule [35]. The hydrogen bond distances are listed in Table 11.

In Table 11 ^{79}Br NQR frequencies are collected for selected temperatures; in case were the measurements gave signals at 77 K and at 295 K, these temperatures have preference in Table 11. In Table A.4 we list the coefficients for the parameterization of the temperature dependence of $\nu(^{79}Br)$ according to

$$\nu = \sum_{i=-1}^{2} a_i T^i. \tag{1}$$

L-Cysteine hydrobromide monohydrate, L-Cys · HBr · H_2O

The crystal structure of L-Cys · HBr · H_2O is reported in this paper. Searching for the Br NQR spectrum within $11 \leq \nu/\text{MHz} \leq 41$, two NQR signals were detected. The frequency ratio is 1.1970 ($\nu(^{79}Br)/\nu(^{81}Br)$). In agreement with the structure there is only one crystallographically independent $Br^{\ominus}$ ion in the unit cell. $\nu(^{79}Br) = f(T)$ is plotted in Figure 9. The

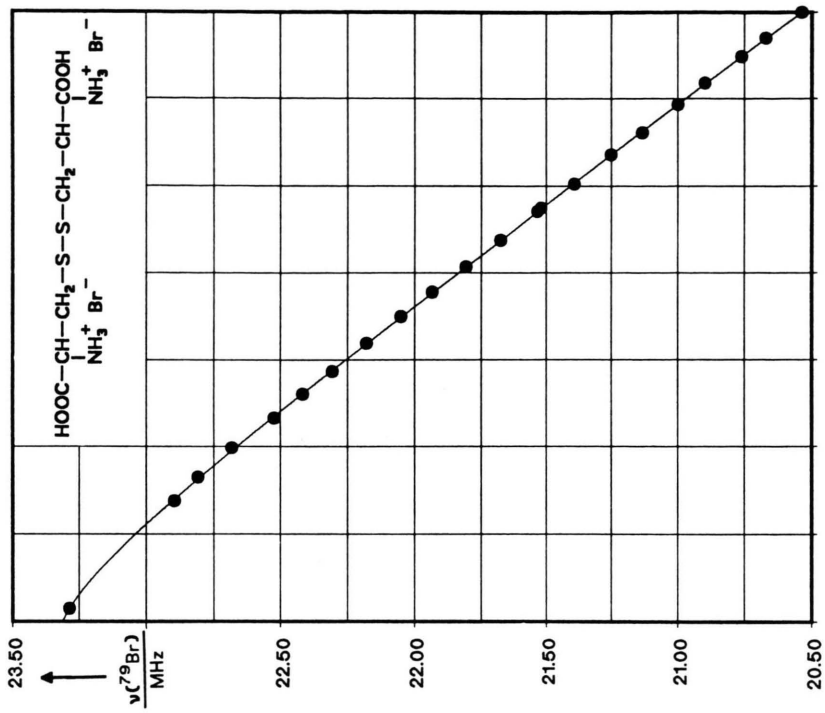

Fig. 10. ^{79}Br NQR singlet of L-cystine dihydrobromide as a function of temperature.

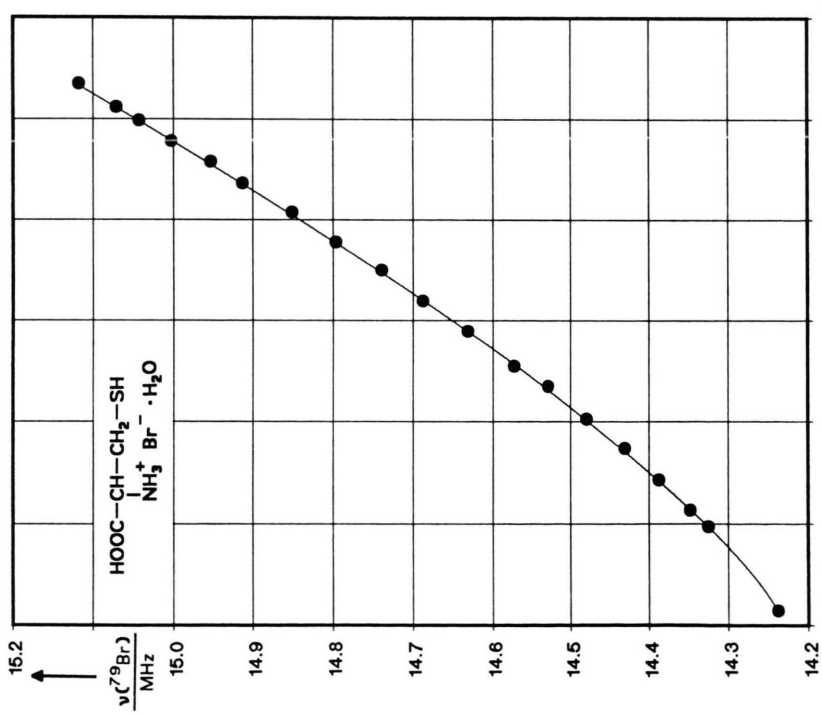

Fig. 9. ^{79}Br NQR singlet of L-cysteine hydrobromide monohydrate as a function of temperature.

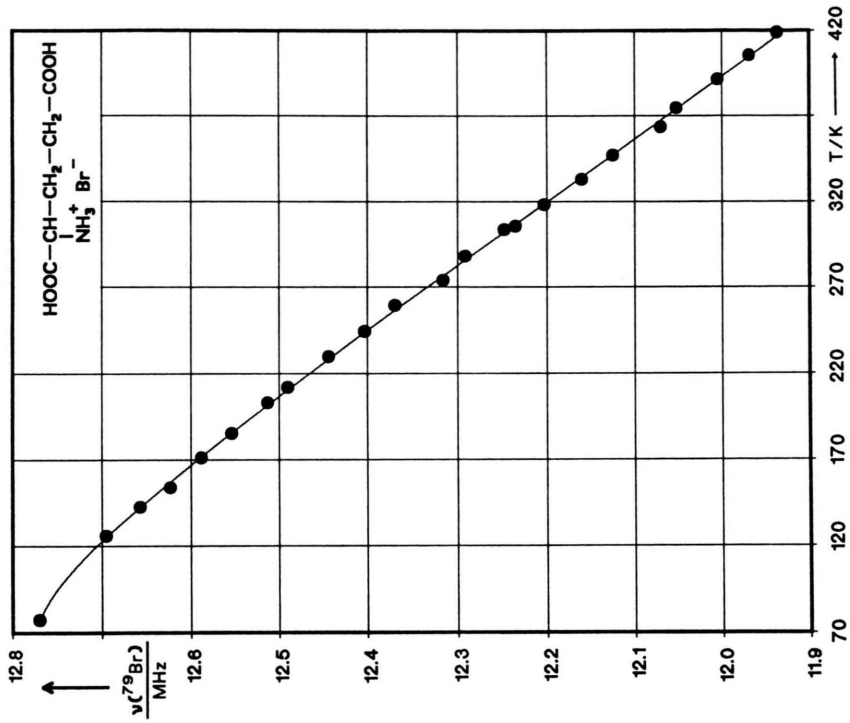

Fig. 12. ^{79}Br NQR singlet of L-glutamic acid as function of temperature.

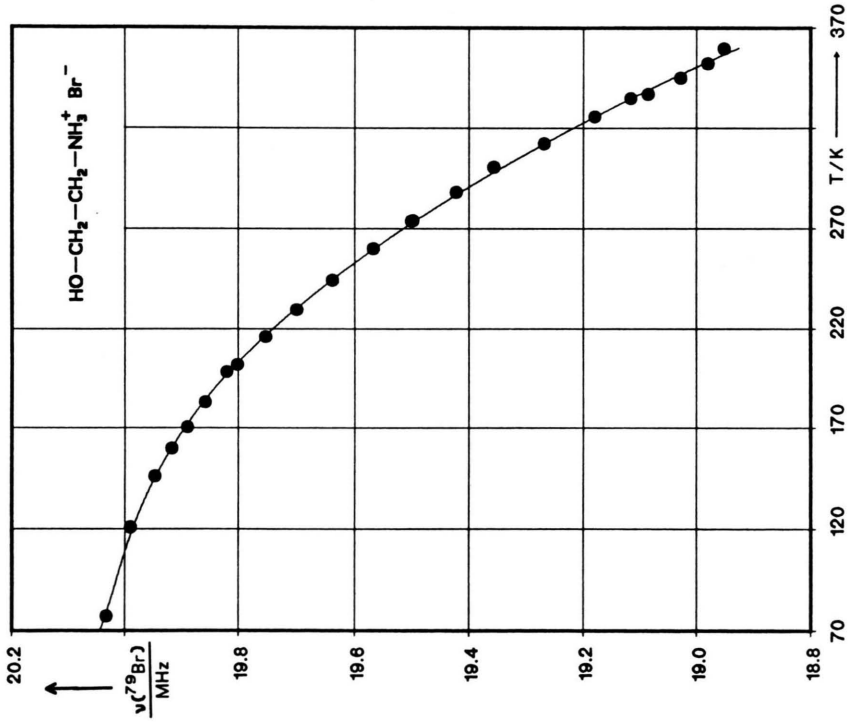

Fig. 11. ^{79}Br NQR singlet of ethanolamine as function of temperature.

temperature dependence is "anomalous" if one considers a negative temperature coefficient predicted by the Bayer theory as "normal" [37]. $\nu(T)$ is nearly linear over the whole range covered, $77 \leq T/K \leq 341$ (T_m). At 77 K the frequency is 14.238 MHz with an S/N of 7. S/N increases to 40 at 171 K, decreasing from thereon to 10 at 337 K. For selected frequencies see Table 11, for the parameterization of $\nu(^{79}Br) = f(T)$ see Table A.4.

There is neither a simple explanation for the positive temperature coefficient of the ^{79}Br NQR frequency in L-Cys · HBr · H_2O nor for the maximum in S/N at 171 K. Most probably the dynamics of the hydrogen bond system may be responsible for these observations.

L-Cystine dihydrobromide, L-Cys-S-S-L-Cys · 2 HBr

In the range $10 \leq \nu/MHz \leq 28$, at room temperature, a Br NQR dublet was observed, one line at 18.224 MHz, the other one at 21.809 MHz. The ratio of the frequencies, 1.1967, corresponds to the known ratio of the nuclear quadrupole moments of ^{79}Br and ^{81}Br. The dependence of the ^{79}Br NQR frequency was studied in the range $77 \leq T/K \leq 420$, see Figure 10. Selected frequencies are found in Table 11, and the parameterization of $\nu(^{79}Br) = f(T)$ is listed in Table A.4. A negative temperature coefficient, almost constant, is observed. No phase transition appears, neither in $\nu(^{79}Br) = f(T)$ nor in the DTA (the latter one in the range $77 \leq T/K \leq 479$). The ^{79}Br singlet shows only one crystallographically independent bromine in the unit cell of L-Cys-S-S-L-Cys · 2 HBr.

Crystallizing L-Cys-S-S-L-Cys · 2 HBr from solution rapidly, a dihydrate is formed [38]; its crystal structure is known, monoclinic, $P2_1$, $Z=2$ [39], involving two crystallographically inequivalent bromines. Crystals we have grown under such conditions did not give an NQR signal.

The structure of the waterfree compound, we have studied, is known, orthorhombic, $P2_122_1$ [40–43]. The cystine molecule is built up from two cysteine units, connected through a disulfide bridge. The hydrobromide is isostructural with L-Cys-S-S-L-Cys · 2 HCl [44–46]. There is only one bromine point position in the unit cell, in agreement with NQR. Four hydrogen bonds are directed towards the bromine ion, three of the type $N-H \cdots Br^{\ominus}$, one of the type $O-H \cdots Br^{\ominus}$. The distances $A \cdots D$ are listed in Table 12.

Table 12. Hydrogen bond distances Acceptor A ··· Donor D in L-cystine dihydrobromide [42] and ethanolamine hydrobromide [47].

Compound	L-Cys-S-S-L-Cys · 2 HBr	$HOCH_2CH_2NH_3^{\oplus}Br^{\ominus}$
Connection	$d(A \cdots D)/pm$	$d(A \cdots D)/pm$
$A \cdots D$		
$Br \cdots O$	317	340
$Br \cdots N'$	328	339
$Br \cdots N''$	342	340
$Br \cdots N'''$	341	329

Ethanolamine hydrobromide

Here we deal not with an amino acid, but there is the possibility of both hydrogen bond connections, $N-H \cdots Br^{\ominus}$, and $O-H \cdots Br^{\ominus}$. $HOCH_2CH_2NH_2$ is the reduced form of glycine. Searching within $10 \leq \nu/MHz \leq 25$, a NQR dublet was observed with the frequency ratio 1.1967. Only one crystallographic independent bromine is in the unit cell of $HOCH_2CH_2NH_2 \cdot HBr$, confirming the crystal structure determination [47] (triclinic, $P\bar{1}$).

In Fig. 11 $\nu(^{79}Br) = f(T)$ is shown; $d\nu(^{79}Br)/dT$ is normal, negative. No phase transition is visible in the diagram $\nu(^{79}Br) = f(T)$ and no sign of it was observed in the DTA ($77 \leq T/K \leq 360$). S/N of the signal is 15 at 77 K, increasing to 100 at 200 K and then decreasing to 7 at 360 K. At room temperature S/N is 75. The ^{79}Br NQR frequency is 19.5 MHz at 273 K, somewhat low for a hydrogen bond coordination of three $N-H \cdots Br^{\ominus}$ bonds and one $O-H \cdots Br^{\ominus}$ bond. The acceptor–donor distances for the title compound are given in Table 12. About selected frequencies and the parameters a_i of (1) see Table 11 and Table A.4, respectively.

L-Glutamic acid hydrobromide, L-Glu · HBr

Two Br NQR signals were detected at room temperature in the range $8 \leq \nu/MHz \leq 38$ and the frequency ratio is 1.1969, i.e. the ratio of the nuclear quadrupole moments $Q(^{79}Br)/Q(^{81}Br)$. The temperature dependence of $\nu(^{79}Br)$ is plotted in Figure 12. $d\nu/dT$ is negative and no phase transition shows up in Figure 12. S/N increases from 4 at 77 K to 12 at 420 K. For selected frequencies see Table 11, and for the parameterization of $\nu(T)$ see Table A.4. L-Glu · HBr crystallizes with the space group $P2_12_12_1$, $Z=4$ [48, 49], having one crystallographically independent bromine in the unit cell, in agreement with NQR. The com-

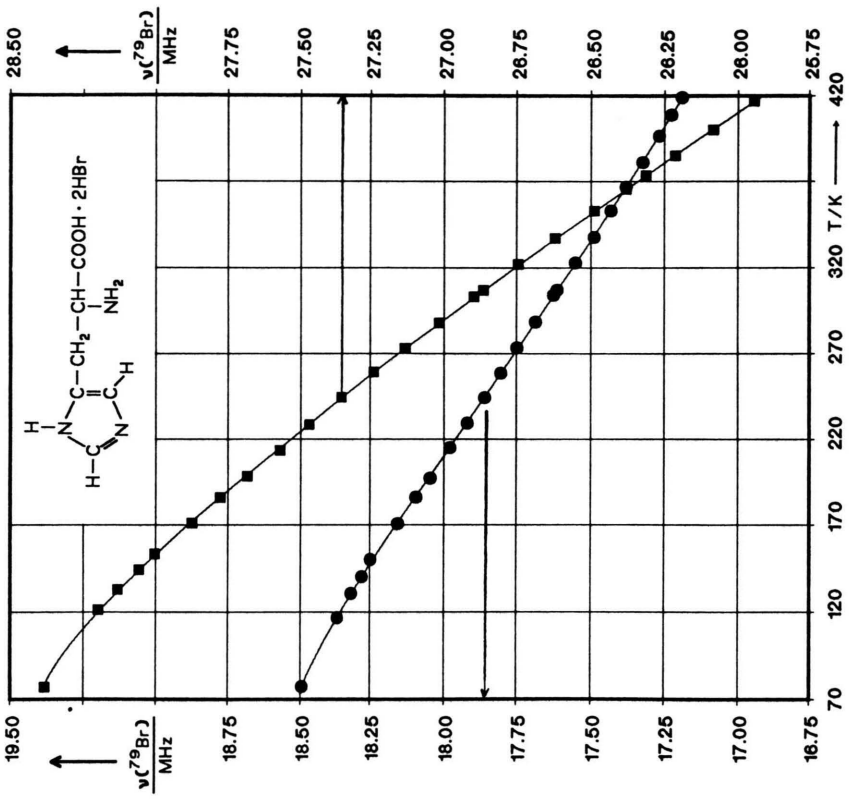

Fig. 14. L-histidine dihydrobromide, $\nu(^{79}\mathrm{Br}) = f(T)$.

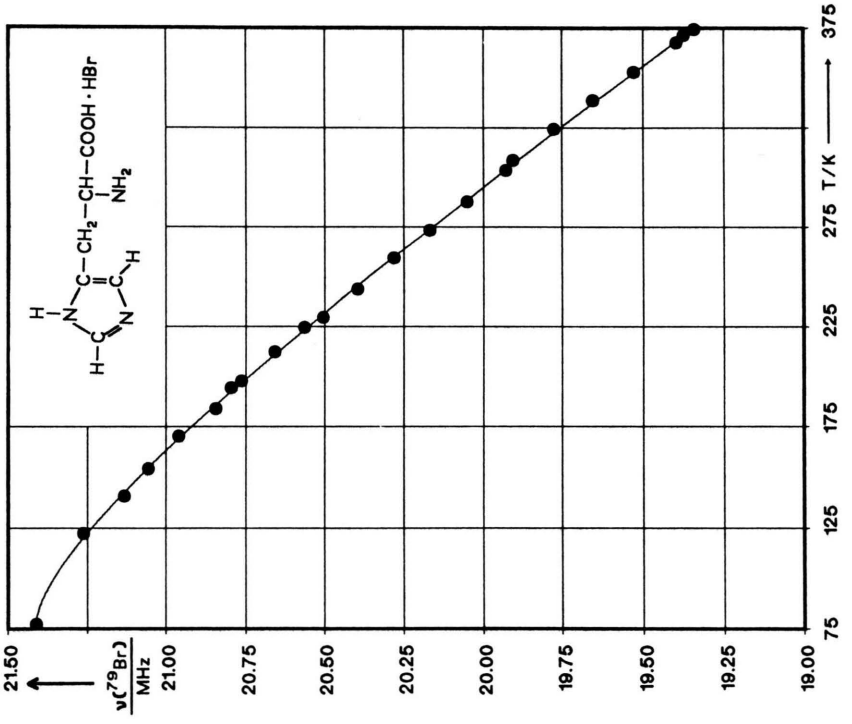

Fig. 13. $\nu(^{79}\mathrm{Br}) = f(T)$ for L-histidine hydrobromide.

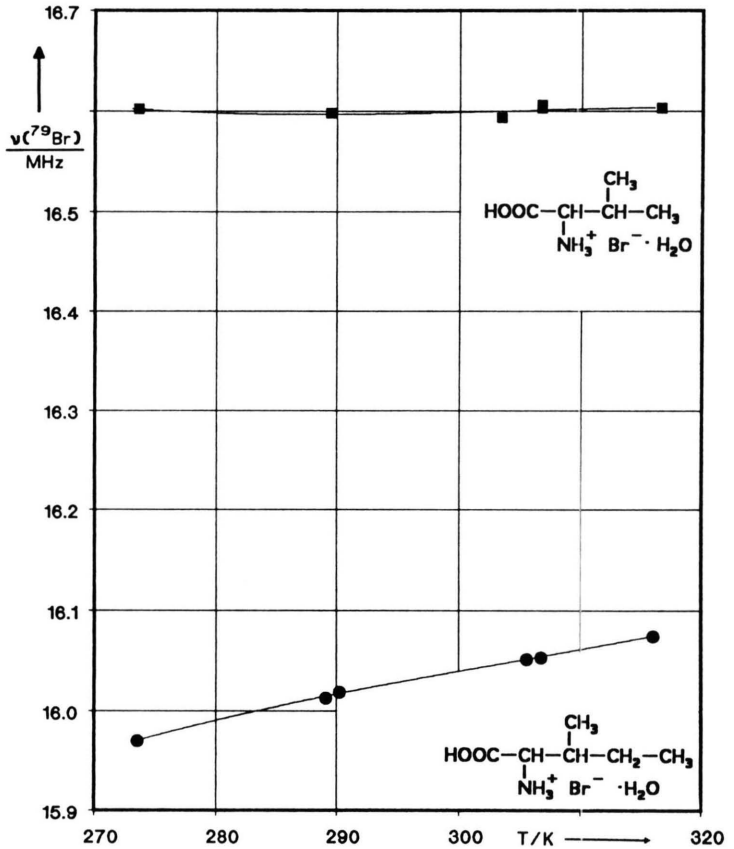

Fig. 15. The temperature dependence of the ^{79}Br NQR spectrum of L-isoleucine hydrobromide monohydrate and L-valine hydrobromide monohydrate.

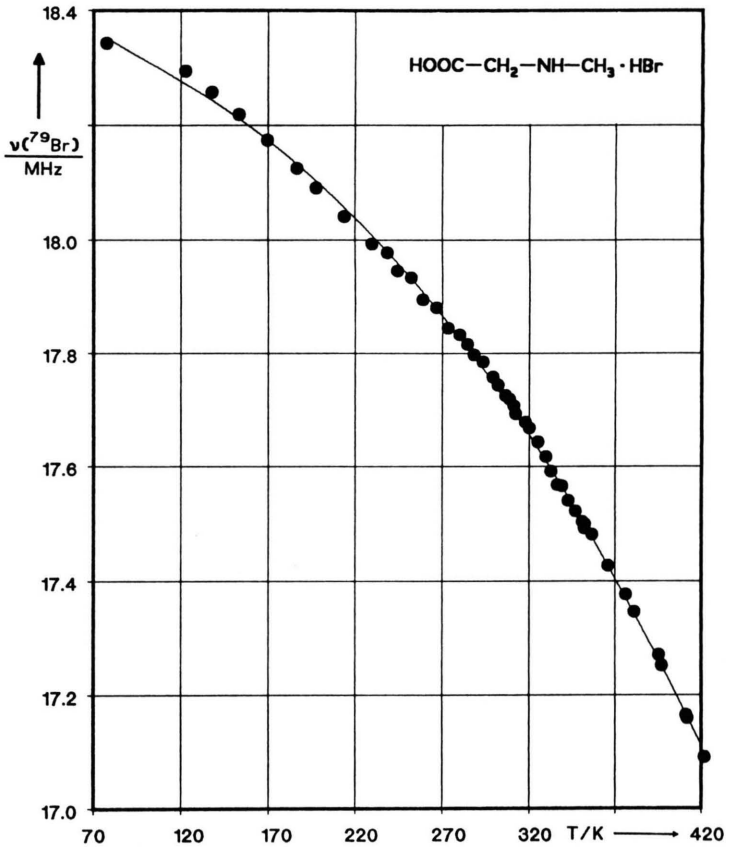

Fig. 16. $\nu(^{79}\mathrm{Br}) = f(T)$ of sarcosine hydrobromide as function of temperature.

pound is isostructural with the hydrochloride, L-Glu · HCl [48, 50, 51] as the complete solid state miscibility of L-Glu · HBr and L-Glu · HCl has shown, and with the hydroiodide, L-Glu · HI [52]. The very low ^{79}Br NQR frequency of 12 MHz at 273 K indicates according to our model either a pure N–H ··· $Br^{\ominus}$ hydrogen bond system, as it was found for L-Glu · HI, or a system of two O–H ··· $Br^{\ominus}$ bonds and two N–H ··· $Br^{\ominus}$ bonds. For L-Glu · HCl two N–H ··· $Br^{\ominus}$ bonds and one O–H ··· $Br^{\ominus}$ bond have been found [50]. In L-Glu · HI the ^{127}I NQR frequencies are also quite low ($\nu_1 = 13.37$ MHz, $\nu_2 = 24.18$ MHz at 273 K) [53]. We assume that the hydrogen bond arrangement in L-Glu · HBr is similar to L-Glu · HI.

L-Histidine hydrobromide, L-His · HBr

Crystallisation of L-His · HBr from aqueous solution at room temperature yields large, waterclear, multifaced crystals with xH_2O. Since we could not find any ^{79,81}Br NQR spectrum in the range 10 MHz to 25 MHz at room temperature, the compound was not further investigated. On heating the compound to 373 K, H_2O is lost irreversibly. A sample, dried at 403 K to constant weight and annealed, gave in the NQR search, $10 \leq \nu/\text{MHz} \leq 28$, two signals which belong to one bromine point position. The temperature dependence of the ^{79}Br NQR singlet is normal, see Figure 13; no phase transition occurs. DTA from 77 K to 513 K (T_{mp}) confirms the one phase behavior. S/N shows a maximum around 240 K. Selected frequencies are found in Table 11, and the parameterization of $\nu(T)$ is given in Table A.4. The crystal structure of L-His · HBr is not known, and from the ^{79}Br frequency, being around 19.95 MHz at room temperature, one cannot speculate about the hydrogen bond system.

L-Histidine dihydrobromide, L-His · 2 HBr

The crystal structure of L-His · 2 HBr is reported in the present paper. Searching for NQR lines within $8 \leq \nu/\text{MHz} \leq 32$, we observed four signals, separable into two pairs by applying the frequency relation between the ^{79}Br and ^{81}Br; $\nu_{1,2}(^{79}\text{Br})/\nu_{1,2}(^{81}\text{Br}) = 1.1967$ is found. The NQR dublet of ^{79}Br is plotted as a function of temperature in Figure 14. The low frequency line at 17.75 MHz ($T = 273$ K) can be assigned to the bromine with N–H ··· $Br^{\ominus}$ surrounding only. The high frequency line, 27.13 MHz at 273 K, belongs to the bromine ion which has an O–H ··· $Br^{\ominus}$ bond besides the N–H ··· $Br^{\ominus}$ bonds. This is an obvious application of our model, in conformity with the crystal structure. Of course, a unic proof has to come from single crystal Zeeman split NQR experiments. Worth mentioning is the temperature coefficient of the NQR frequencies: that of the upper line is almost twice that of the lower one. Over the whole temperature range covered, S/N of the lower frequency line is practically twice that of the higher frequency line. Together with the difference in the temperature coefficients, this is an interesting point to work on; most probably it is a question of molecular dynamics in the lattice. There is no sign of a phase transition neither in the NQR spectrum nor in the DTA (77 K to 420 K). For selected frequencies and the parameterization of $\nu(^{79}\text{Br}) = f(T)$, see Table 11 and Table A.4.

L-Isoleucine hydrobromide monohydrate, L-Ile · HBr · H_2O;
L-Valine hydrobromide monohydrate, L-Val · HBr · H_2O

Both, L-Ile and L-Val are amino acids with an aliphatic side chain, branching at the atom $C^{(\beta)}$. Two Br NQR signals were found in both compounds, and in both cases the frequencies had a ratio of 1.1969. We can assume that in the unit cells of both compounds there is only one bromine in the asymmetric unit. In Fig. 15 the ^{79}Br NQR frequencies are plotted against the temperature. $d\nu/dT$ is quite small and S/N is small in both cases. Only in a restricted temperature range we could observe the signals.

The structure of D-Ile · HBr · H_2O is known [32], and therefore we know the structure of L-Ile · HBr · H_2O, $P2_12_12_1$, $Z = 4$. The hydrogen bond system is composed of one N–H ··· $Br^{\ominus}$ bond, which is donated from the ammonium group. Then there are three O–H ··· $Br^{\ominus}$ bonds, one of them due to OH of the COOH group and two of them donated by H_2O (by different molecules). The surrounding of the bromine ion in L-Ile · HBr · H_2O is similar to that found in L-Cys · HBr · H_2O.

The crystal structure of L-Val · HBr · H_2O is not known. By DTA we observed a reversible phase transition with T_c of 318 K (increasing temperature) and 242 K (decreasing temperature). The ^{79}Br NQR frequency is favourable for $Br^{\ominus}$ with N–H ··· $Br^{\ominus}$ bonds only or with two N–H ··· $Br^{\ominus}$ bonds and two O–H ··· $Br^{\ominus}$ bonds.

Sarcosine hydrobromide, Sar · HBr

In the range 10–25 MHz one ^{79}Br NQR line was observed. The frequency course with temperature is smooth, the temperature coefficient negative, no sign of a phase transition, neither from the NQR experiment nor from DTA (77 K–435 K). S/N is high, 80 at 77 K, decreasing to 50 at 120 K, increasing again up to 80 at 190 K from where it goes down to 5 at 422 K. From the ^{79}Br NQR frequency we expect similar circumstances for the hydrogen bond scheme as the ones we discussed for L-Val · HBr · H_2O. But one of these possibilities cannot be realized because only one O–H bond per $Br^{\ominus}$ is available. In Fig. 16 $\nu(^{79}\mathrm{Br}) = f(T)$ is plotted; selected frequencies are given in Table 11, and the power series development of $\nu(^{79}\mathrm{Br}) = f(T)$ is listed in Table A.4.

Disarcosine hydrobromide, $(Sar)_2$ · HBr

The crystal structure determination of the orthorhombic $(Sar)_2$ · HBr, space group $Pca2_1$, showed two crystallographically independent bromine ions in the unit cell [54]. Accordingly, in the search for NQR four lines have been observed in the range $11 \leq \nu/\mathrm{MHz} \leq 25$, a dublet for ^{81}Br and a dublet for ^{79}Br. $Br^{(1)}$ experiences two hydrogen bonds N–H $\cdots$ $Br^{\ominus}$, $Br^{(2)}$ three such bonds, and the two ^{79}Br lines should be in the low frequency range, where they are observed. Selected frequencies and parameters of the power series development of $\nu(^{79}\mathrm{Br}) = f(T)$ are given in Table 11 and Table A.4, respectively. In Fig. 17 $\nu(^{79}\mathrm{Br}) = f(T)$ is plotted. We cannot assign the two frequencies to the bromine positions in the unit cell. The upper line is observable within a limited range (233–314 K) and S/N is low (2–5). S/N for the lower frequency is small, too (≤ 7). Neither NQR nor DTA ($77 \leq T/\mathrm{K} \leq 380$) shows any sign of a phase transition of $(Sar)_2$ · HBr.

Glycine lithium bromide, Gly · LiBr;
Glycyl-glycine lithium bromide, (Gly-Gly) · LiBr

Within this study we became interested in the interaction of hydrogen bonds with the halide ions in compounds of alkali metal halides with amino acids. We studied the series Gly · LiBr, (Gly-Gly) · LiBr, and (Gly-Gly-Gly) · LiBr, because for the two latter ones crystal structure data are available [55, 56]. Only for the two former salts NQR signals could be found. At 295 K the following results have been found: Gly · LiBr, $\nu(^{79}\mathrm{Br}) = 16.850$ MHz; S/N = 7; (Gly-Gly) · LiBr, $\nu(^{79}\mathrm{Br}) = 17.873$ MHz, S/N = 10. The resonance frequencies fit well into the range we propose for a coordination of $Br^{\ominus}$ with hydrogen bonds N–H $\cdots$ $Br^{\ominus}$ only, and this is preferred in the crystal structure of (Gly-Gly) · LiBr. It may be worthwhile to look by NQR more closely into the bond scheme of alkali halide double salts with amino acids and peptides.

^{127}I NQR

Ethanolamine hydroiodide

Several hydroiodides of amino acids have been investigated here, see Table 1. In the search for ^{127}I NQR the range $10 \leq \nu/\mathrm{MHz} \leq 39$ was covered and two resonance lines were found, corresponding to the two transitions ν_1 ($m = \pm 1/2 \leftrightarrow m = \pm 3/2$) and ν_2 ($m = \pm 3/2 \leftrightarrow m = \pm 5/2$) of the $I = 5/2$ nucleus ^{127}I. Using the solution of the secular equation given in [57], $e\Phi_{zz}Qh^{-1}(^{127}\mathrm{I})$ and the asymmetry parameter $\eta(^{127}\mathrm{I})$ can be calculated. At $T = 273$ K for ethanolamine $\nu_1(^{127}\mathrm{I}) = 16.074$ MHz, $\nu_2(^{127}\mathrm{I}) = 19.406$ MHz. Therefrom $e\Phi_{zz}QH^{-1}(^{127}\mathrm{I}) = 70.715$ MHz and $\eta(^{127}\mathrm{I}) = 0.7773$ is calculated. In Fig. 18 the temperature dependence of ν_1 and ν_2 is plotted and Fig. 19 shows the functions $e\Phi_{zz}Qh^{-1}(^{127}\mathrm{I}) = f(T)$ and $\eta(^{127}\mathrm{I}) = f(T)$. S/N of $\nu_1(^{127}\mathrm{I})$ decreases from 90 at 77 K to 18 at 130 K, increasing then to 140 at 303 K and then decreasing again. A similar course of S/N (ν_2) is observed. On the basis of the measured nuclear quadrupole coupling constant, NQCC, only N–H $\cdots$ $I^{\ominus}$ bonds should be present around the iodine ion in the crystal. However, this assumption is somewhat uncertain because of the few examples with simultaneous knowledge of structure and NQR spectrum of hydroiodides.

Sarcosine hydroiodide, Sar · HI

Using a sample crystallized from aqueous solution by evaporation of the solvent, two ^{127}I NQR signals have been detected at room temperature in the range $10 \leq \nu/\mathrm{MHz} \leq 43$. $\nu_1^{\mathrm{I}}(^{127}\mathrm{I})$ at 20.62 MHz, $\nu_2^{\mathrm{I}}(^{127}\mathrm{I})$ at 35.76 MHz. $e\Phi_{zz}Qh^{-1}(^{127}\mathrm{I}) = 122.008$ MHz, $\eta(^{127}\mathrm{I}) = 0.3519$ follows therefrom. Only one iodine will be in the asymmetric unit of the unit cell of phase I of Sar · HI. Crystallizing a sample from the melt, a dif-

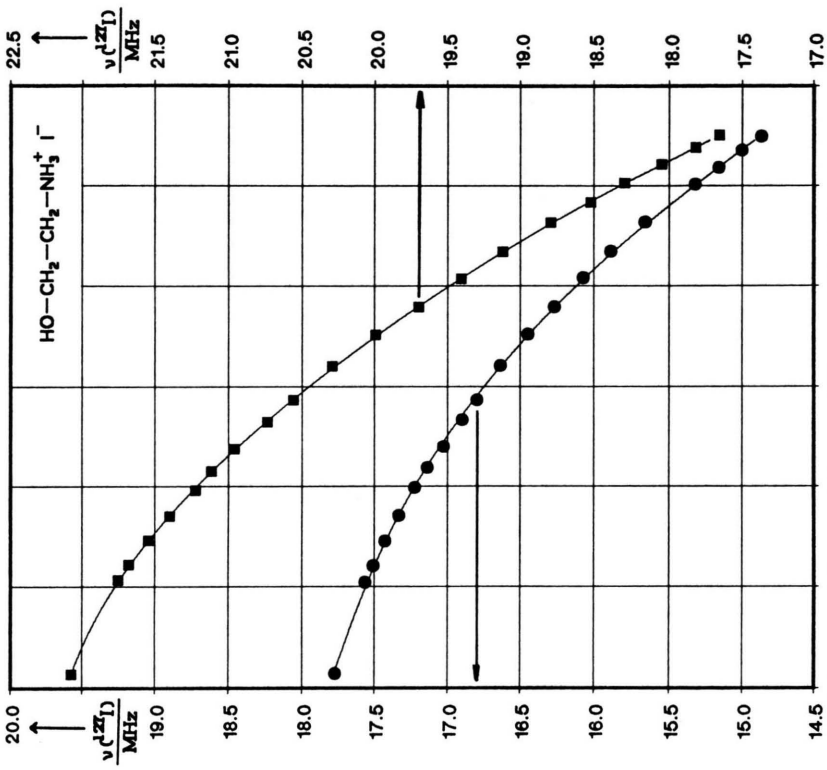

Fig. 18. Ethanolamine hydroiodide: The ^{127}I NQR frequencies ν_1 and ν_2 as functions of temperature.

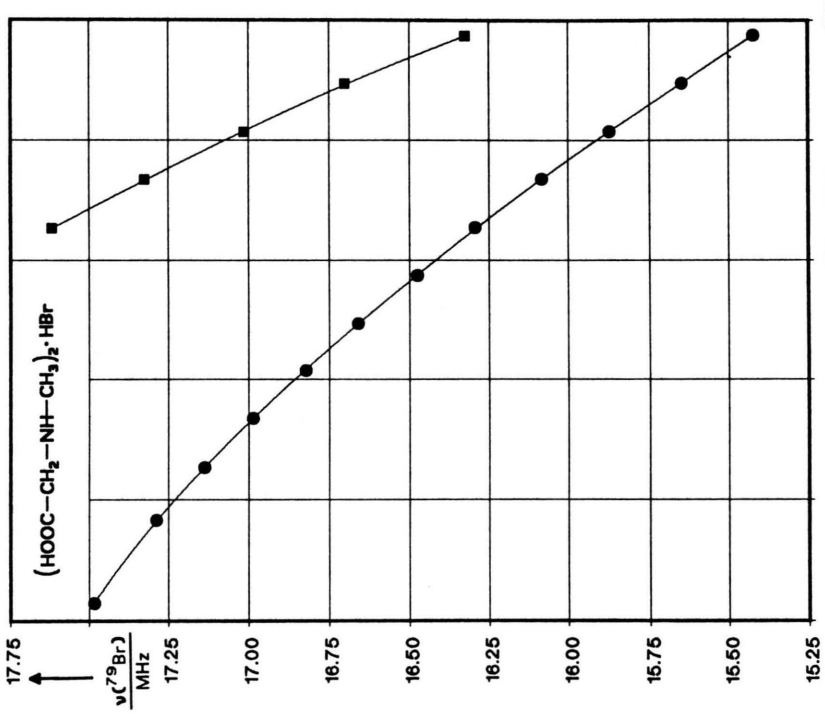

Fig. 17. Disarcosine hydrobromide, $(Sar)_2 \cdot HBr$; temperature dependence of the ^{79}Br NQR spectrum.

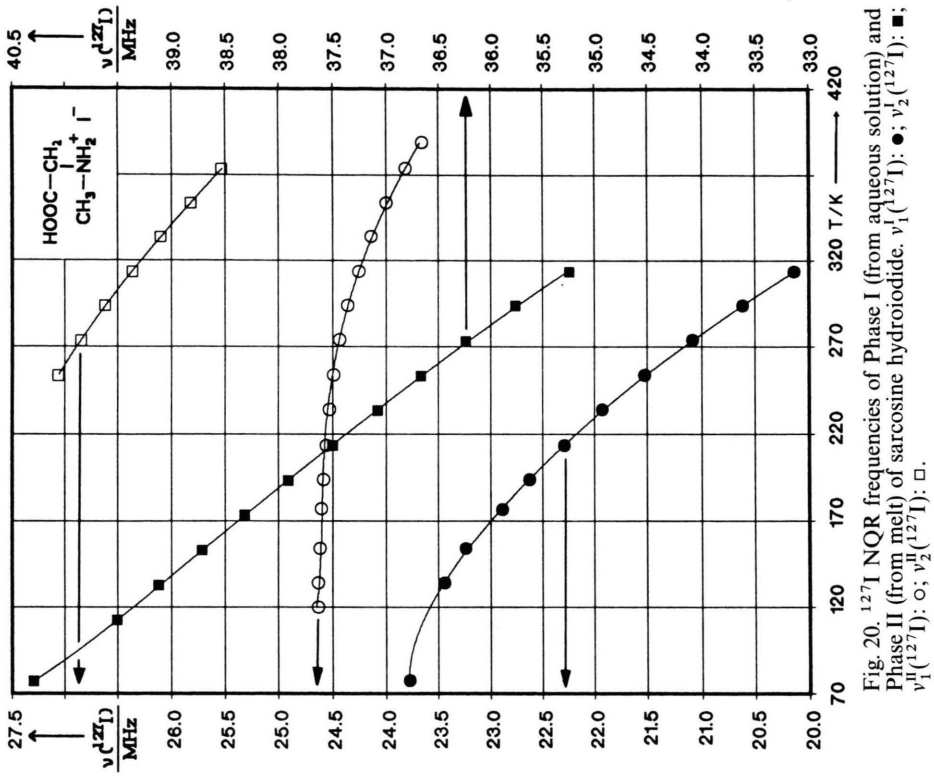

Fig. 20. ^{127}I NQR frequencies of Phase I (from aqueous solution) and Phase II (from melt) of sarcosine hydroiodide. $\nu_1^{I}(^{127}I)$: ●; $\nu_2^{I}(^{127}I)$: ■; $\nu_1^{II}(^{127}I)$: ○; $\nu_2^{II}(^{127}I)$: □.

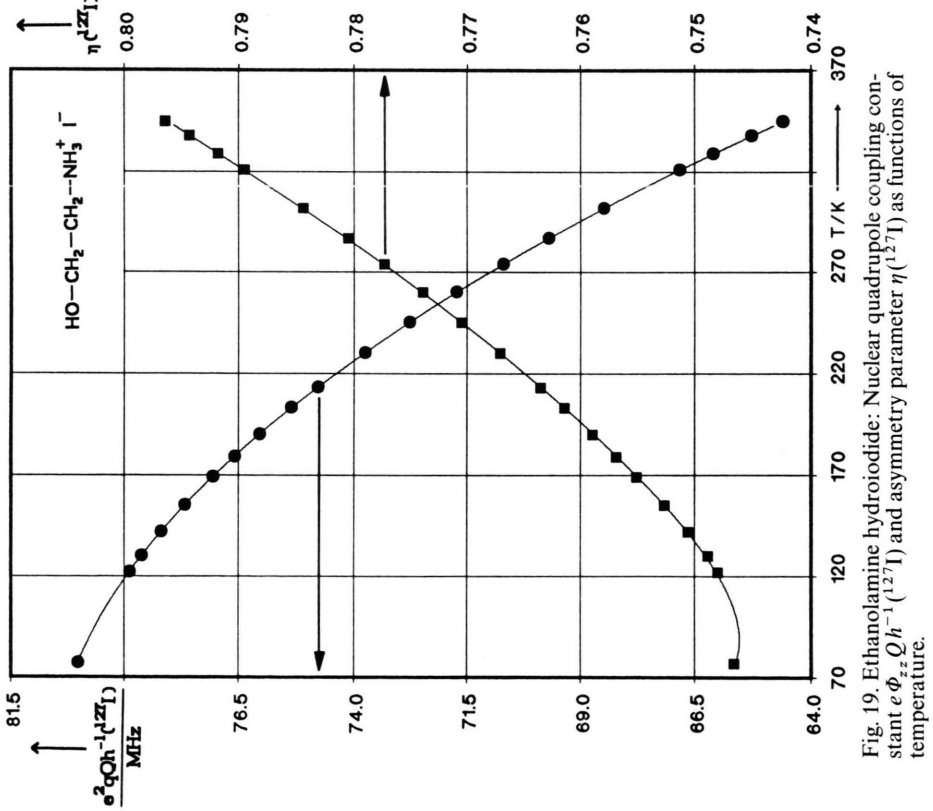

Fig. 19. Ethanolamine hydroiodide: Nuclear quadrupole coupling constant $e\Phi_{zz}Qh^{-1}(^{127}I)$ and asymmetry parameter $\eta(^{127}I)$ as functions of temperature.

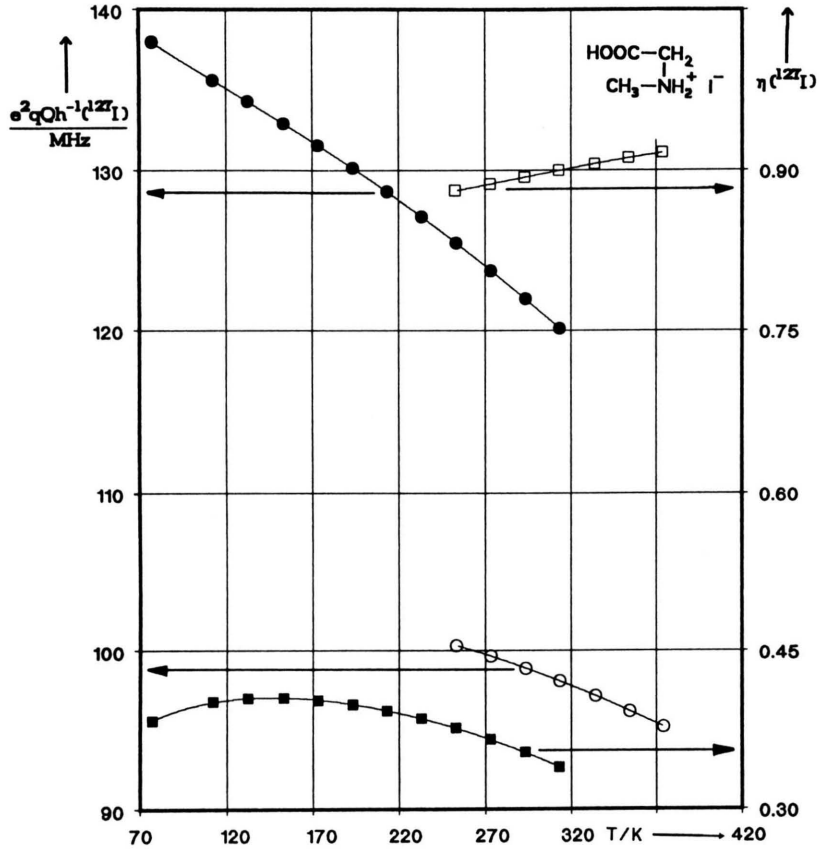

Fig. 21. $e\Phi_{zz}Qh^{-1}(^{127}\mathrm{I})$ and $\eta(^{127}\mathrm{I})$ of Phase I and Phase II of sarcosine hydroiodide as functions of temperature. $e\Phi_{zz}Qh^{-1}(^{127}\mathrm{I})^{\mathrm{I}}$: ●; $\eta(^{127}\mathrm{I})^{\mathrm{I}}$: ■; $e\Phi_{zz}Qh^{-1}(^{127}\mathrm{I})^{\mathrm{II}}$: ○; $\eta(^{127}\mathrm{I})^{\mathrm{II}}$: □.

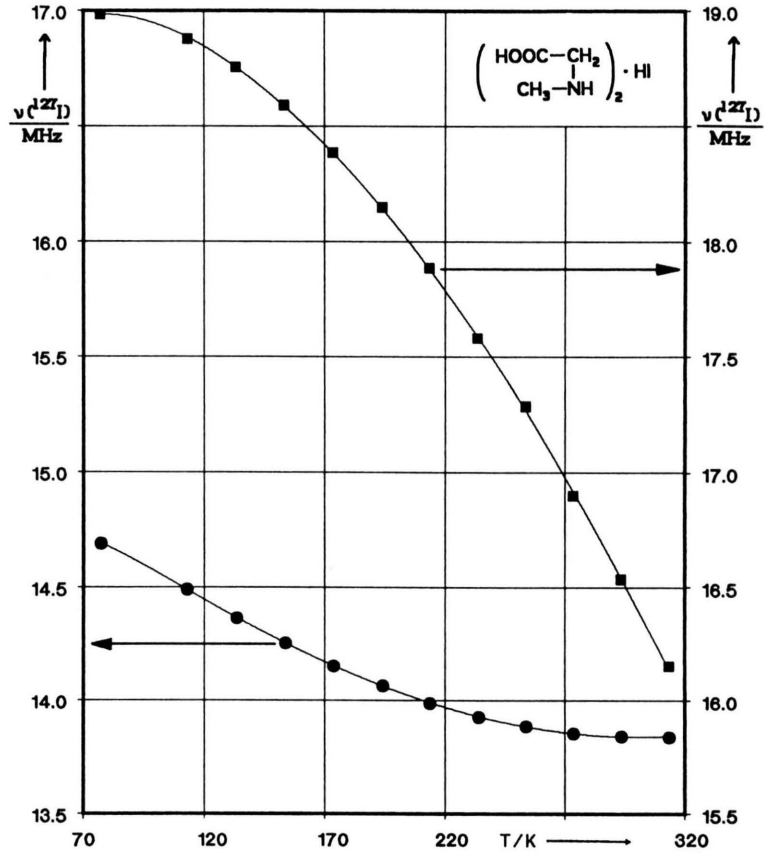

Fig. 22. Temperature dependence of the ^{127}I NQR frequencies of disarcosine hydroiodide.

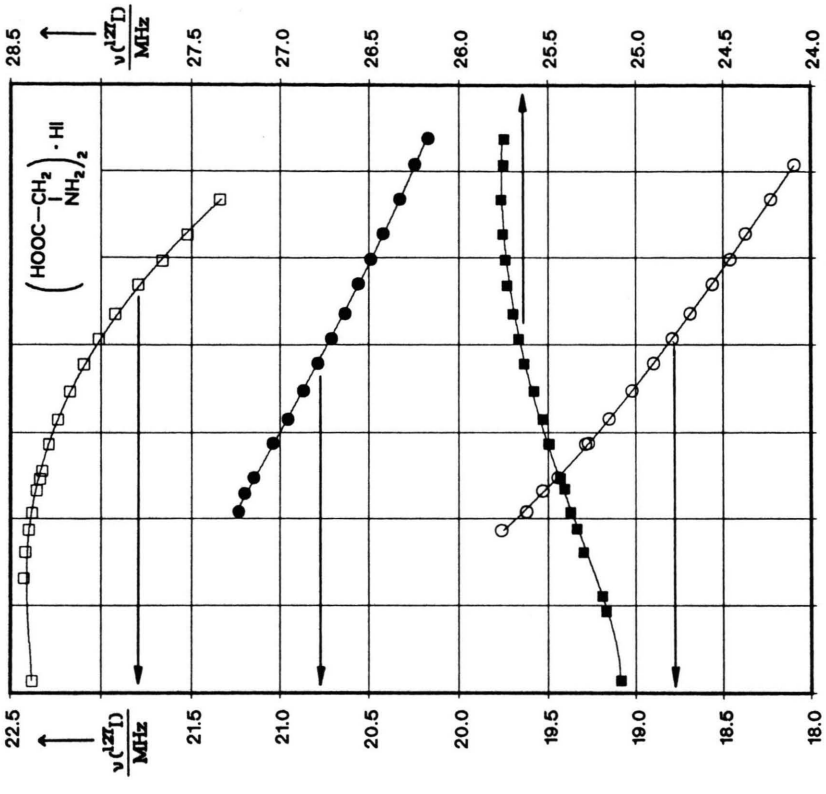

Fig. 24. ^{127}I NQR frequencies of diglycine hydroiodide, temperature dependence.

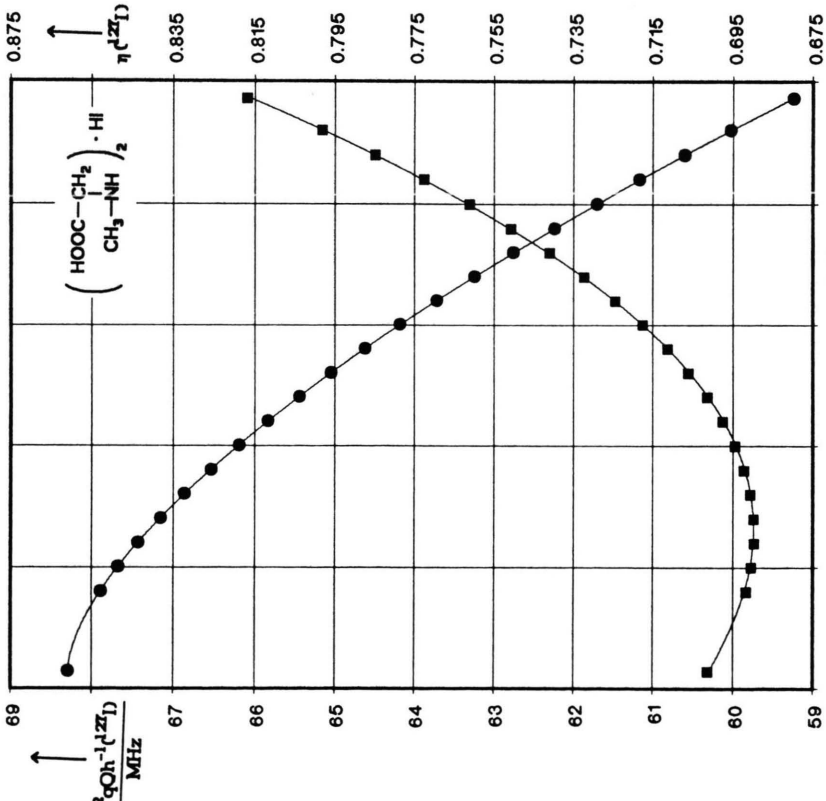

Fig. 23. $e\Phi_{zz}Qh^{-1}$ (^{127}I) and η(^{127}I) of disarcosine hydroiodide as functions of temperature.

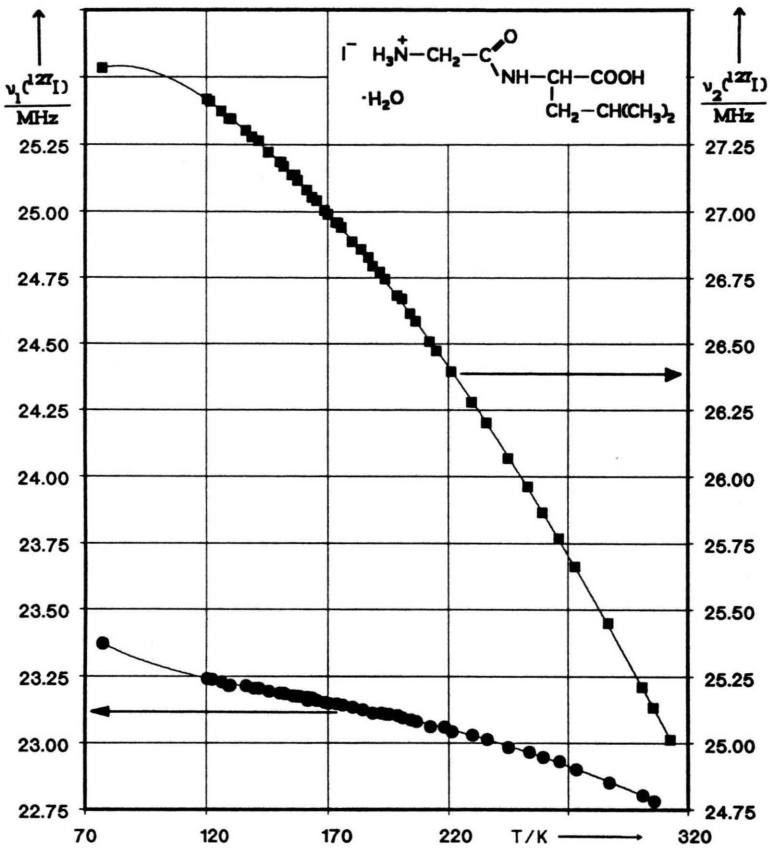

Fig. 25. Temperature dependence of the ^{127}I NQR frequencies of glycyl-L-leucine hydroiodide monohydrate.

ferent ^{127}I NQR spectrum is observed with $\nu_1^{II}(^{127}I) = 24.263$ MHz, $\nu_2^{II}(^{127}I) = 26.620$ MHz at room temperature; $e\Phi_{zz}Qh^{-1}(^{127}I) = 98.911$ MHz, $\eta(^{127}I) = 0.8933$. We call this phase II. In NQR $= f(T)$ and DTA ($77 \leq T/K \leq 442$ (T_m)) there was no phase transition observable, neither from phase I to phase II nor from II to I. At the time being, the relation between phase I and phase II is not known. Unfortunately, no information on the crystal structure of Sar · HI is available. In Fig. 20 the ^{127}I NQR frequencies are plotted in their dependence on temperature for both phases, and in Fig. 21 such a plot is shown for the NQCC (^{127}I) and for $\eta(^{127}I)$. Frequencies, NQCC and η are found in Table 11; the coefficients of the parameterization are listed in Table A.4.

Disarcosine hydroiodide, $(Sar)_2 \cdot HI$

In the search for ^{127}I NQR at 293 K, the range $10 \leq \nu/MHz \leq 38$ was covered and two signals were detected, $\nu_1(^{127}I) = 13.843$ MHz, $\nu_2(^{127}I) = 16.535$ MHz. We conclude: In the unit cell of $(Sar)_2 \cdot HI$ there is only one iodine in the asymmetric unit. $e\Phi_{zz}Qh^{-1}(^{127}I) = 60.813$ MHz, $\eta(^{127}I) = 0.785$ is calculated for $T = 290$ K. Both frequencies are given as a function of T in Fig. 22 and $e\Phi_{zz}Qh^{-1}(^{127}I) = f(T)$ and $\eta(^{127}I) = f(T)$ are shown in Figure 23. As before, selected frequencies etc. are given in Table 11, the coefficients of (1) in Table A.4. No phase transition could be detected by DTA ($77 \leq T/K \leq 419$). On the basis of the rule: hydrogen bond scheme around the halogen ion and resonance frequency, respectively NQCC, we assume pure $N-H \cdots I^{\ominus}$ coordination. This is supported by the composition of the compound; there is only one chance for an $O-H \cdots I^{\ominus}$ bond (from the COOH group) but four possibilities for $N-H \cdots I^{\ominus}$ bonds (two $-(NH_2CH_3)^{\oplus}$ groups).

Diglycine hydroiodide, $(Gly)_2 \cdot HI$

The crystal structure of $(Gly)_2 \cdot HI$ is available [58]. The monoclinic crystal has two crystallographically

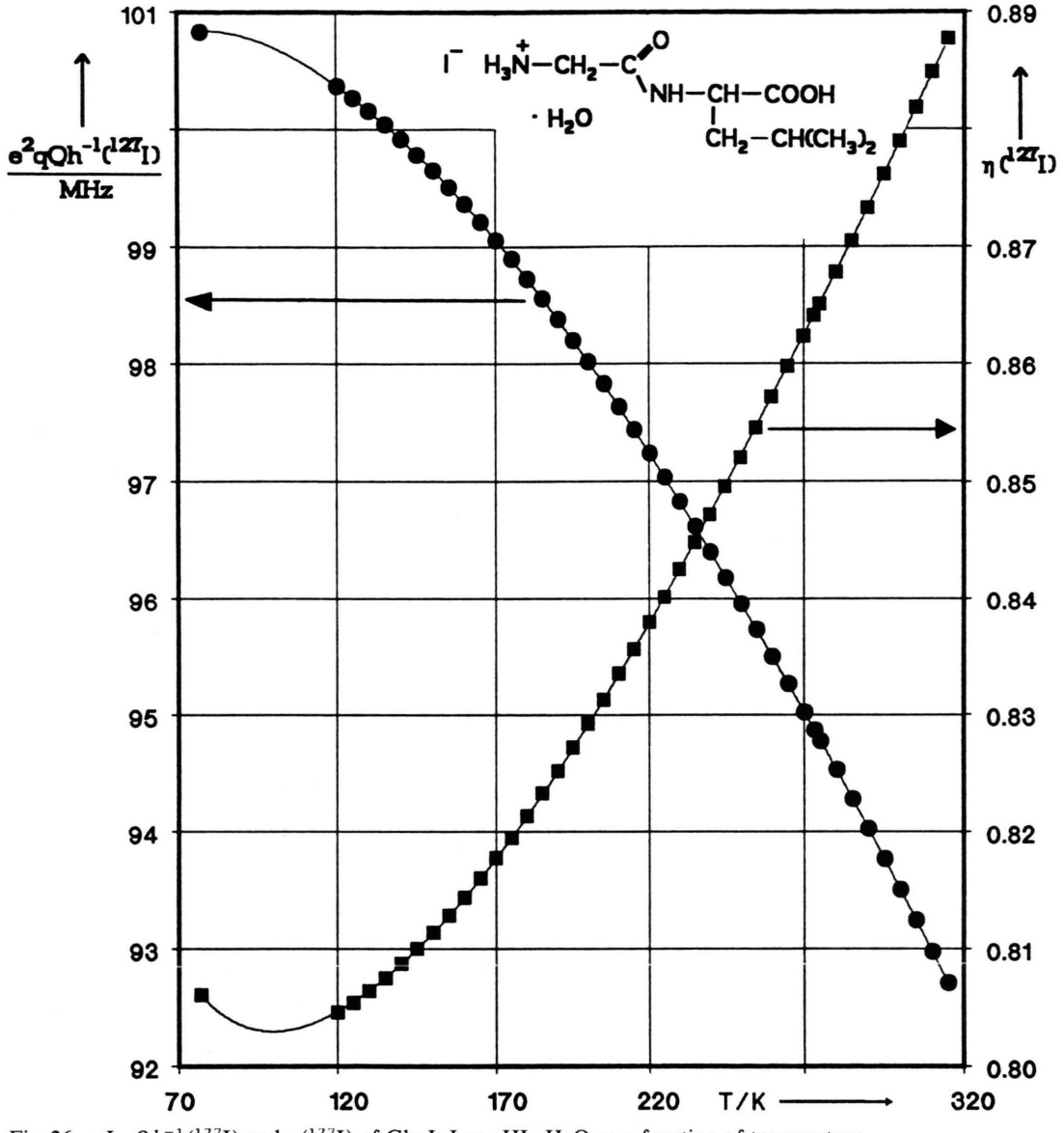

Fig. 26. $e\Phi_{zz}Qh^{-1}(^{127}I)$ and $\eta(^{127}I)$ of Gly-L-Leu · HI · H_2O as a function of temperature.

independent iodine ions in the unit cell, C2, $Z=8$. Both iodines have a similar hydrogen bond coordination of four bonds N–H $\cdots$ $I^{\ominus}$, differing in geometry and bond length. As expected from the crystal structure, in the range $10 \leq \nu/\text{MHz} \leq 48$ four ^{127}I NQR lines are observed: $\nu_1(^{127}I) = 18.692$ MHz; $\nu_2(^{127}I) = 20.638$ MHz; $\nu_3(^{127}I) = 21.921$ MHz, $\nu_4(^{127}I) = 25.694$ MHz ($T = 288$ K). Looking on the I $\cdots$ N distances [58] one expects only little differences in $e\Phi_{zz}Qh^{-1}(^{127}I)$ for $I^{(1)}$ and $I^{(2)}$, and this is reflected by the small range one finds the four resonances in. In Fig. 24 $\nu_{1,2,3,4}(^{127}I)$ are plotted as functions of temperature. On the basis of the frequencies only, there is no chance to assign a certain pair to one iodine. Also the temperature dependence is of no help and neither S/N, which is rather low (≤ 10) and similar for the four lines. Using the possible combinations one finds $76.02 \leq e\Phi_{zz}Qh^{-1}(^{127}I) \leq 91.83$ and $0.879 \leq \eta(^{127}I) \leq 0.926$. Since, in any case, $\eta(^{127}I)$ is high, we searched for the transition $m \pm 1/2 \rightarrow m = \pm 5/2$, but without success. A double resonance experiment with simultaneous excitation of both transitions would be

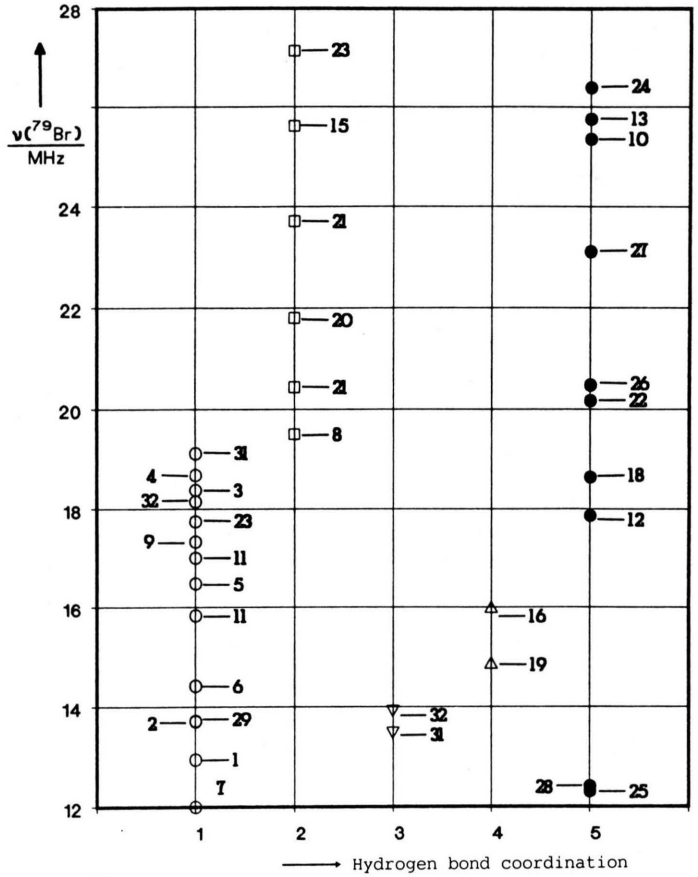

Fig. 27. ^{79}Br NQR frequencies of amine- and amino acid hydrobromides at 273 K as a function of the hydrogen bond coordination. 1. Compounds with N–H ··· $Br^{\ominus}$ only. 2. Compounds with N–H ··· $Br^{\ominus}$ and one O–H ··· $Br^{\ominus}$ coordination. 3. Compounds with two N–H ··· $Br^{\ominus}$ bonds and two O–H ··· $Br^{\ominus}$ bonds. 4. Compounds with three O–H ··· $Br^{\ominus}$ bonds and one N–H ··· $Br^{\ominus}$ bond. 5. Compounds for which the crystal structure is not known.

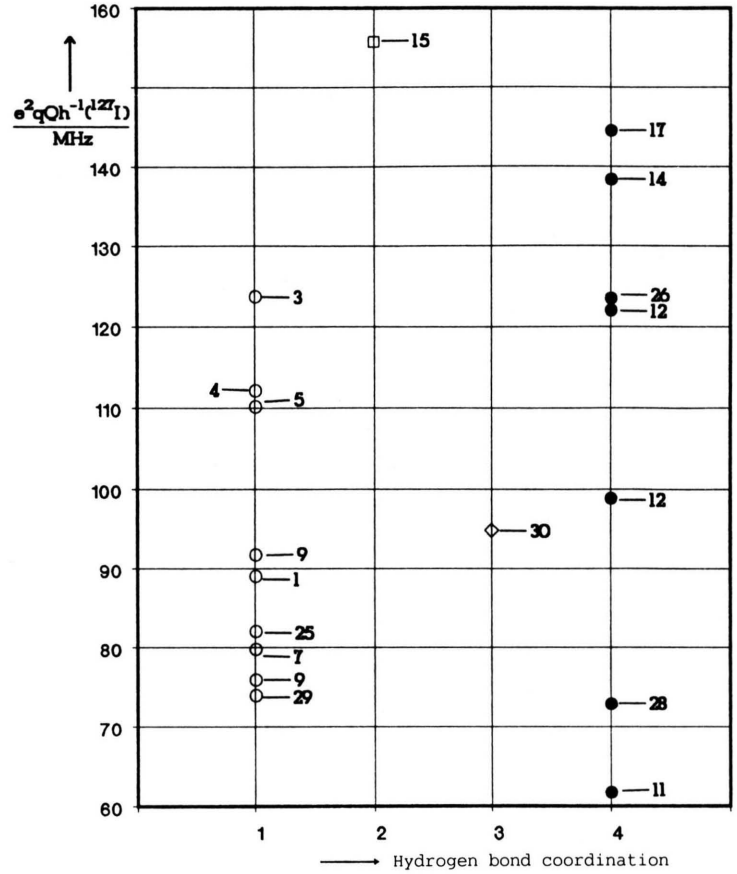

Fig. 28. $e\Phi_{zz}Qh^{-1}(^{127}\mathrm{I})$ as a function of the hydrogen bond geometry at the iod atom in amine- and amino acid hydroiodides. 1. Compounds with N–H ··· $I^{\ominus}$ coordination only. 2. Compounds with N–H ··· $I^{\ominus}$ hydrogen bonds plus one O–H ··· $I^{\ominus}$ bond. 3. Compounds with two N–H ··· $I^{\ominus}$ bonds and two O–H ··· $I^{\ominus}$ bonds. 4. The coordination is unknown; no crystal structure available.

a possibility to solve the problem of assignment (or a single crystal experiment).

Di-L-Valine hydroiodide, (L-Val)$_2$ · HI

Only preliminary measurements of ^{127}I NQR were done on (L-Val)$_2$ · HI. We just give the results at $T = 295$ K. (L-Val)$_2$ · HI: $\nu_1(^{127}\mathrm{I}) = 34.00$ MHz, $\nu_2(^{127}\mathrm{I}) = 37.27$ MHz, $e\Phi_{zz}Qh^{-1}(^{127}\mathrm{I}) = 138.396$ MHz, $\eta(^{127}\mathrm{I}) = 0.8895$.

Glycyl-L-leucine hydroiodide monohydrate, Gly-L-Leu · HI · H_2O

The last compound, we report in this paper NQR data for, is Gly-L-Leu · HI · H_2O, the crystal structure of which is given above. The spectrum shows two NQR lines, as expected from the structure work. At 289 K one finds $\nu_1(^{127}\mathrm{I}) = 22.854$; $\nu_2(^{127}\mathrm{I}) = 25.449$ MHz, therefrom $e\Phi_{zz}Qh^{-1}(^{127}\mathrm{I}) = 94.036$ MHz, $\eta(^{127}\mathrm{I}) = 0.8733$. Fig. 25 shows $\nu = f(T)$, Fig. 26 the dependence of $e\Phi_{zz}Qh^{-1}(^{127}\mathrm{I})$ and $\eta(^{127}\mathrm{I})$ on T. S/N goes with temperature through a maximum (45 at 253 K); ν_2 has a maximum in S/N too, at the same temperature but a factor of 1.5 higher. No phase transition was observed. There are (see Table 8) two N–H ··· I$^{\ominus}$ bonds and two O–H ··· I$^{\ominus}$ bonds coordinating the iodine ion. For the hydrobromides we have proposed [2] that the NQR frequencies are lowered by going from the coordination: one O–H ··· Br$^{\ominus}$ bond to two O–H ··· Br$^{\ominus}$ bonds; here we find that this rule holds for iodides, too.

Discussion

By the formation of hydrogen bonds (donor) D–H ··· A (acceptor) with amido- or ammonium groups or the hydroxyl group as the donating groups, N–H ··· X, O–H ··· X, X = halogen, the structure and cohesion in the solid state of amino acid hydrohalides is determined. This is true also for di-, tri-, ... peptides. A criterion for the formation of hydrogen bonds are the van der Waals radii of the atoms A and D. If the distance A ··· D is smaller than the sum $r_{vdw}(A) + r_{vdw}(D)$, the existence of hydrogen bonds can be assumed (geometrical criterion [59–61, 3]). With knowledge of the hydrogen position, the criterion is stronger; the distance D ··· A should be smaller than the sum of covalent distance D–H and $r_{vdw}(H) + r_{vdw}(A)$ [62]. Here we list r_{vdw} (in pm) of the atoms D and A and of H as used in this paper. There are small differences in the radii given by Pauling [63] and Bondi [64].

Atom	r_{vdw} [63]	r_{vdw} [64]	Atom	r_{vdw} [63]	r_{vdw} [64]
H	120	120	Cl	180	175
N	150	155	Br	195	185
O	140	152	I	215	198

For alkylamine and amino acid hydrobromides we have proposed [1] a correlation between the ^{79}Br NQR frequency and the kind of hydrogen bonds attacking at the bromine site. If only N–H ··· Br$^{\ominus}$ coordinates the bromine ion, the range in which the ^{79}Br NQR frequencies are found is $12 \leq \nu(^{79}\mathrm{Br})/\mathrm{MHz} \leq 20$; if in the hydrogen bond coordination of the bromine ion an additional O–H ··· Br$^{\ominus}$ bond is present, the frequency range is shifted upwards to $19.5 \leq \nu(^{79}\mathrm{Br})/\mathrm{MHz} \leq 27.5$ (at $T = 273$ K [2]). In Fig. 27 we show the ^{79}Br NQR data of the present investigation, together with literature data, divided into 5 groups according to the coordination of hydrogen bonds around the ion Br$^{\ominus}$. The data on which this figure is based are given in Table A.5. It is clearly seen that the frequency range for $\nu(^{79}\mathrm{Br})$ is $12 \leq \nu(^{79}\mathrm{Br})/\mathrm{MHz} \leq 19.5$. One O–H ··· Br$^{\ominus}$ bond besides the N–H ··· Br$^{\ominus}$ bond shifts the frequencies up into the range $19.5 \leq \nu(^{79}\mathrm{Br})/\mathrm{MHz} \leq 29$. Introduction of a more symmetrical surrounding, which can be assumed with a coordination of two N–H ··· Br$^{\ominus}$ bonds and two O–H ··· Br$^{\ominus}$ bonds, lowers the range to 13–14 MHz; unfortunately the experimental material is meager for this situation. Three O–H ··· Br$^{\ominus}$ bonds and one N–H ··· Br$^{\ominus}$ bond leads to low ^{79}Br NQR frequencies, too. We cannot assign the frequencies plotted in column 5 of Fig. 27 to a coordination; the coordination is unknown.

The picture for the dependence of $e\Phi_{zz}Qh^{-1}(^{127}\mathrm{I})$ from the coordination of hydrogen bonds around the iodine ion gives a similar impression as Fig. 28 shows. The column for the coordination three O–H ··· I$^{\ominus}$ bonds, one N–H ··· I$^{\ominus}$ bond is missing; we have no example. The ranges we find on the basis of the available material are $72 \leq e\Phi_{zz}Qh^{-1}(^{127}\mathrm{I})/\mathrm{MHz} \leq 125$ for pure N–H ··· I$^{\ominus}$ coordination, $150 \leq e\Phi_{zz}Qh^{-1}(^{127}\mathrm{I})/\mathrm{MHz} \leq 160$ for one O–H ··· I$^{\ominus}$ bond included in the coordination, and $e\Phi_{zz}Qh^{-1}(^{127}\mathrm{I})$ around 95 MHz if two O–H ··· I$^{\ominus}$ bonds and two N–H ··· I$^{\ominus}$ bonds form the surrounding of the ion I$^{\ominus}$. No doubt, there

is not enough experimental material available to make the predictions more precise.

The criticism, we have to face for the qualitative estimates we give, is as follows.

a) In case of the ^{79}Br NQR frequencies, there may be some modification of Fig. 27 if $e\Phi_{zz}Qh^{-1}(^{79}\text{Br})$ would be available. From single crystal work on Gly-L-Ala · HBr · H_2O we know that $\eta(^{79}\text{Br})$ is large (around 83%) [5, 74]. To switch for Br ($I(^{79,81}\text{Br}) = 3/2$) from $\nu(^{79}\text{Br})$ to $e\Phi_{zz}Qh^{-1}(^{79}\text{Br})$ needs a rather involved experiment, impossible without single crystals.

b) A second point is our treatment of the hydrogen bond influence on NQR frequencies simply by coordination. We only differentiate between $O-H\cdots X^{\ominus}$ bonds and $N-H\cdots X^{\ominus}$ bonds. In a first approximation this is a reasonable approach as Figs. 27 and 28 show. Progress will be possible by considering the detailed geometry of the coordination, bond lengths and angles, calculating or estimating a charge distribution over the atoms N, O, and H and calculating the EFG by an extended point charge model [75]. The latter one has to take into account that we are dealing with solids belonging to some extent to the group of ionic solids. The lattice charges have an influence on the EFG as found out from single crystal studies [74]. This influence becomes stronger with increasing polarizability of the halogen ion (Cl → Br → I).

Acknowledgement

We are grateful to the Deutsche Forschungsgemeinschaft and to the Fonds der Chemie for support of this work.

[1] S. Fleck and Al. Weiss, Ber. Bunsenges. Phys. Chem. **88,** 956 (1984).
[2] J. Hartmann, S.-q. Dou, and Al. Weiss, Ber. Bunsenges. Phys. Chem. **94,** 1110 (1990).
[3] G. C. Pimentel and A. L. McClellan, Ann. Rev. Phys. Chem. **22,** 347 (1971).
[4] A. Kehrer, S. Fleck, and Al. Weiss, Ber. Bunsenges. Phys. Chem. **91,** 1176 (1987).
[5] A. Kehrer, Dr.-Ing. Dissertation, Darmstadt 1991.
[6] G. M. Sheldrick, SHELX86. Program for crystal structure solution. University of Göttingen, Germany 1986.
[7] G. M. Sheldrick, SHELX76. Program for crystal structure determination. University of Cambridge, England 1976.
[8] T. J. Kistenmacher and T. Sorell, Cryst. Struct. Commun. **2,** 673 (1973).
[9] T. J. Kistenmacher and T. Sorell, J. Cryst. Mol. Struct. **4,** 419 (1974).
[10] J. Donohue, I. R. Lavine, and J. S. Rollett, Acta Cryst. **9,** 655 (1956).
[11] J. Donohue and A. Caron, Acta Cryst. **17,** 1178 (1964).
[12] K. Oda and H. Koyama, Acta Cryst. **B 28,** 639 (1972).
[13] B. Evertsson, Acta Cryst. **B 25,** 30 (1969).
[14] I. Bennett, A. G. H. Davidson, M. M. Harding, and I. Morelle, Acta Cryst. **B 26,** 1722 (1970).
[15] T. N. Bhat and M. Vijayan, Acta Cryst. **B 34,** 2556 (1978).
[16] J. J. Madden, E. L. McGandy, and N. C. Seeman, Acta Cryst. **B 28,** 2377 (1972).
[17] M. S. Lehman, T. F. Koetzle, and W. C. Hamilton, Int. J. Pept. Prot. Res. **4,** 229 (1972).
[18] J. J. Madden, E. L. McGandy, N. C. Seeman, M. M. Harding, and A. Hoy, Acta Cryst. **B 28,** 2382 (1972).
[19] P. Edington and M. M. Harding, Acta Cryst. **B 30,** 204 (1974).
[20] R. E. Marsh and J. Donohue, Adv. Protein Chem. **22,** 235 (1967).
[21] E. Benedetti, in: 5th Amer. Pept. Symp. (M. Goodman and J. Meierhofer, eds.). Wiley & Sons, New York 1977, p. 257.
[22] R. Ramachandra Ayyar and R. Srinivasan, Curr. Sci. **34,** 449 (1965).
[23] R. Ramachandra Ayyar, Z. Kristallogr. **126,** 227 (1968).
[24] K. A. Kerr and J. P. Ashmore, Acta Cryst. **B 29,** 2124 (1973).
[25] K. A. Kerr and J. P. Ashmore, Acta Cryst. **B 31,** 2022 (1975).
[26] M. M. Harding and H. A. Long, Acta Cryst. **B 24,** 1096 (1968).
[27] I. C. Paul, in: The Chemistry of the Thiol Group, Part 1, 111 (S. Patai, ed.), J. Wiley & Sons, London 1974.
[28] V. Pattabhi, K. Venkatesan, and S. R. Hall, J. Chem. Soc. Perkin II, 1722 (1974).
[29] E. Subramanian, Acta Cryst. **22,** 910 (1967).
[30] M. O. Chaney, O. Seely, and L. K. Steinrauf, Acta Cryst. **B 27,** 544 (1971).
[31] S. Thyagaraja Rao, Z. Krist. **129,** 50 (1969).
[32] J. Trommler and J. M. Bijvoet, Acta Cryst. **7,** 703 (1954).
[33] S. K. Mazumdar and R. Srinivasan, Curr. Sci. **33,** 573 (1964).
[34] S. K. Mazumdar, Indian J. Pure Appl. Phys. **3,** 411 (1965).
[35] S. K. Mazumdar and R. Srinivasan, Z. Krist. **123,** 186 (1966).
[36] K. K. Chacko and S. K. Mazumdar, Z. Krist. **128,** 315 (1969).
[37] H. Bayer, Z. Phys. **130,** 227 (1951).
[38] M. J. Colaneri and H. C. Box, J. Chem. Phys. **84,** 2926 (1986).
[39] R. E. Rosenfield, Jr. and R. Parthasarathy, Acta Cryst. **B 31,** 816 (1975).
[40] R. Srinivasan, Acta Cryst. **9,** 1039 (1956).
[41] L. K. Steinrauf and L. H. Jensen, Acta Cryst. **9,** 539 (1956).
[42] J. Peterson, L. K. Steinrauf, and L. H. Jensen, Acta Cryst. **13,** 104 (1960).
[43] N. Ananthakrishnan and R. Srinivasan, Indian J. Pure Appl. Phys. **2,** 62 (1964).
[44] L. K. Steinrauf, J. Peterson, and L. H. Jensen, J. Amer. Chem. Soc. **80,** 3825 (1958).
[45] S. C. Gupta, A. Sequeira, and R. Chidambaram, Acta Cryst. **B 30,** 562 (1974).
[46] D. D. Jones, I. Bernal, M. N. Frey, and T. F. Koetzle, Acta Cryst. **B 30,** 1220 (1974).

[47] Ch. H. Koo, Ch. Choe, T. S. Roe, and H. S. Kim, Daehan Hwahak Hwoejee **18,** 25 (1974).
[48] B. Dawson and A. McL Mathieson, Acta Cryst. **4,** 475 (1951).
[49] M. Delfino, G. M. Loiacono, and J. A. Nicolosi, J. Sol. State Chem. **23,** 289 (1978).
[50] B. Dawson, Acta Cryst. **6,** 81 (1953).
[51] A. Sequeira, H. Rajagopal, and R. Chidambaram, Acta Cryst. **B 28,** 2514 (1972).
[52] A. Kirfel and F. Wallrafen, Z. Kristallogr. **171,** 121 (1985).
[53] A. Kehrer, unpublished, Diplomarbeit, TH Darmstadt 1987.
[54] S. C. Battacharyya and N. N. Saha, J. Cryst. Mol. Struct. **8,** 209 (1978).
[55] R. Meulemans, P. Piret, and M. van Meersche, Bull. Soc. Chim. Belges **80,** 73 (1971).
[56] R. Meulemans, P. Piret, and M. van Meersche, Acta Cryst. **B 27,** 1187 (1971).
[57] R. Creel, H. Brooker, and R. G. Barnes, J. Magn. Res. **41,** 146 (1980).
[58] P. Piret, J. Meunier-Piret, and M. van Meersche, Bull. Soc. Chim. Belg. **81,** 539 (1972).
[59] J. M. Robertson and A. L. Ubbelohde, Proc. Roy. Soc. London **A 170,** 222 (1939).
[60] G. C. Pimentel and A. L. McClellan, The Hydrogen Bonding, W. H. Freeman and Co., San Francisco 1960.
[61] W. C. Hamilton and S. A. Ibers, Hydrogen Bonding in Solids, W. A. Benjamin, New York 1968.
[62] Z. Rahim and B. N. Barman, Acta Cryst. **A 34,** 761 (1978).
[63] L. Pauling, The Nature of the Chemical Bond, 3rd ed., Cornell University Press 1960.
[64] A. Bondi, J. Phys. Chem. **68,** 441 (1964).
[65] G. Jugie and J. A. S. Smith, J. Chem. Soc. Faraday Trans. 2, **74,** 994 (1978).
[66] E. F. Gabe, Acta Cryst. **14,** 1296 (1961).
[67] J. J. R. Frausto da Silva and L. F. Vilas Boas, Rev. Port. Quim. **14,** 115 (1972).
[68] F. Mussgnug,. Naturwiss. **29,** 256 (1941).
[69] F. Jellinek, Acta Cryst. **11,** 626 (1958).
[70] M. V. King and W. N. Lipscomb, Acta Cryst. **3,** 222 (1950).
[71] T. Hahn, Z. Kristallogr. **111,** 161 (1959).
[72] A. Kehrer, S.-Q. Dou, and Al. Weiss, Z. Naturforsch. **44a,** 659 (1989).
[73] G. M. Sheldrick and W. S. Sheldrick, Acta Cryst. **B 26,** 1334 (1970).
[74] A. Kehrer, N. Weiden, and Al. Weiss, to be published.
[75] H. M. Maurer, P. C. Schmidt, and Al. Weiss, J. Mol. Struct. **41,** 111 (1977).
[76] IUPAC-IUB Commission on Biochemical Nomenclature, Pure and Appl. Chem. **40,** 293 (1974).
[77] G. N. Ramachandran and V. Sasisekharan, Adv. Protein Chem. **23,** 283 (1968).
[78] A. V. Lakshminarayanan, V. Sasisekharan, and G. N. Ramachandran, Conformation of Biopolymers, Vol. 1.61 (G. N. Ramachandran, ed.), Academic Press, New York 1967.
[79] V. Sasisehkaran and P. K. Ponnuswamy, Biopolymers **9,** 1249 (1970).

Appendix

Table A.1. Point positions and thermal parameters of L-histidine dihydrobromide, $C_6H_{11}Br_2N_3O_2$. All atoms in position 4a of the space group $P2_12_12_1$: x, y, z; $\frac{1}{2}-x, y, \frac{1}{2}+z$; $\frac{1}{2}+x, \frac{1}{2}-y, z$; $x, \frac{1}{2}+y, \frac{1}{2}-z$. The temperature factor is of the form (throughout this paper)

$$T = \exp\{-2\pi^2(U_{11}h^2a^{*2}+U_{22}k^2b^{*2}+U_{33}l^2c^{*2}+2U_{12}hka^*b^*+2U_{13}hla^*c^*+2U_{23}klb^*c^*)\}.$$

U is the isotropic mean for the hydrogen atoms. The U_{ij} are given in pm^2.

Atom	x/a	y/b	z/c	U_{11}, U	U_{22}	U_{33}	U_{12}	U_{13}	U_{23}
$Br^{(1)}$	0.2434(0)	0.2891(0)	0.1844(1)	266(2)	347(2)	440(2)	5(2)	−40(2)	−7(2)
$Br^{(2)}$	0.5118(0)	0.5051(0)	0.7093(0)	319(2)	358(3)	423(2)	−30(2)	−70(2)	85(2)
$C^{(1)}$	0.3084(2)	0.7538(5)	0.1636(5)	228(20)	337(27)	266(19)	−5(21)	−5(16)	33(22)
$C^{(2)}$	0.2690(2)	0.8818(5)	0.1855(7)	289(24)	295(26)	476(23)	3(21)	18(23)	25(26)
$C^{(3)}$	0.1794(3)	0.7050(6)	0.2021(7)	266(26)	560(36)	422(24)	−46(26)	−43(23)	−12(31)
$C^{(4)}$	0.3961(2)	0.7270(6)	0.1300(5)	278(23)	355(27)	286(22)	−8(23)	−4(16)	−6(22)
$C^{(5)}$	0.4412(2)	0.6693(4)	0.3033(6)	229(20)	226(23)	362(21)	−16(19)	24(21)	−28(23)
$C^{(6)}$	0.5316(2)	0.6606(4)	0.2625(5)	291(22)	264(24)	281(22)	3(21)	−46(17)	−6(19)
$N^{(1)}$	0.1879(2)	0.8483(4)	0.2068(6)	271(21)	482(27)	556(23)	109(20)	−40(20)	35(24)
$N^{(2)}$	0.2508(2)	0.6456(4)	0.1751(5)	358(21)	281(21)	338(17)	−23(20)	−53(21)	−19(17)
$N^{(3)}$	0.4276(2)	0.7672(4)	0.4660(4)	216(17)	291(22)	316(18)	1(19)	43(14)	23(18)
$O^{(1)}$	0.5628(1)	0.5587(3)	0.1875(4)	318(15)	323(17)	510(15)	86(14)	26(15)	−97(17)
$O^{(2)}$	0.5689(2)	0.7797(4)	0.3191(5)	213(15)	394(20)	927(23)	−28(16)	73(19)	−207(24)
$H^{(C^{(2)},1)}$	0.2899(24)	0.9831(47)	0.1943(60)	689(143)					
$H^{(C^{(3)},1)}$	0.1315(24)	0.6547(42)	0.2068(51)	401(117)					
$H^{(C^{(4)},1)}$	0.4052(21)	0.6506(43)	0.0160(46)	345(109)					
$H^{(C^{(4)},2)}$	0.4201(24)	0.8269(47)	0.0892(50)	387(124)					
$H^{(C^{(5)},1)}$	0.4207(21)	0.5700(43)	0.3308(54)	389(111)					
$H^{(N^{(1)},1)}$	0.1353(29)	0.9114(52)	0.2498(55)	865(174)					
$H^{(N^{(2)},1)}$	0.2620(25)	0.5465(42)	0.1637(51)	441(125)					
$H^{(N^{(3)},1)}$	0.4586(24)	0.7186(52)	0.5704(50)	600					
$H^{(N^{(3)},2)}$	0.4429(26)	0.8609(52)	0.4326(58)	600					
$H^{(N^{(3)},3)}$	0.3733(26)	0.7501(59)	0.5051(49)	600					
$H^{(O^{(2)},1)}$	0.6203(27)	0.7632(56)	0.3079(64)	751(158)					

Table A.2. Point positions and thermal parameters of L-cysteine hydrobromide monohydrate. $C_3H_{10}BrNO_3S$. All atoms in position 4a of the space group $P2_12_12_1$ see Table A.1. For the definition of the temperature factor see Table A.1, too.

Atom	x/a	y/b	z/c	U_{11}, U	U_{22}	U_{33}	U_{12}	U_{13}	U_{23}
$Br^{(1)}$	0.3598(0)	0.5515(0)	0.0196(1)	460(1)	260(1)	380(1)	3(1)	17(1)	39(1)
$C^{(1)}$	0.4520(1)	−0.0270(4)	0.7086(6)	280(12)	366(14)	387(16)	40(11)	−48(11)	−6(14)
$C^{(2)}$	0.3871(1)	0.0835(3)	0.7454(5)	313(11)	276(12)	274(14)	−1(10)	−27(10)	13(11)
$C^{(3)}$	0.3664(1)	0.1844(3)	0.5167(5)	303(10)	274(10)	340(14)	−14(8)	−17(13)	33(12)
$N^{(1)}$	0.3286(1)	−0.0319(3)	0.8162(5)	335(10)	336(12)	371(13)	35(9)	71(10)	90(12)
$O^{(1)}$	0.3142(1)	0.1573(3)	0.4095(4)	453(10)	549(12)	606(16)	−158(9)	−219(10)	289(13)
$O^{(2)}$	0.4129(1)	0.3036(2)	0.4567(5)	433(9)	410(10)	424(13)	−131(8)	−61(10)	137(11)
$O^{(w)}$	0.2646(1)	0.7531(2)	0.4498(4)	373(9)	318(9)	493(14)	−21(7)	76(10)	12(11)
$S^{(1)}$	0.4502(0)	−0.1714(1)	0.4458(2)	461(3)	450(4)	468(5)	63(3)	55(4)	−103(4)
$H^{(C^{(1)}, 1)}$	0.4899(14)	0.0453(39)	0.6885(58)	600(0)					
$H^{(C^{(1)}, 2)}$	0.4617(12)	−0.0980(36)	0.8690(60)	600(0)					
$H^{(C^{(2)}, 1)}$	0.3929(12)	0.1670(36)	0.8953(58)	600(0)					
$H^{(N^{(1)}, 1)}$	0.2929(13)	0.0431(39)	0.8657(58)	600(0)					
$H^{(N^{(1)}, 2)}$	0.3398(13)	−0.0964(37)	0.9365(61)	600(0)					
$H^{(N^{(1)}, 3)}$	0.3127(13)	−0.1042(38)	0.6635(61)	600(0)					
$H^{(O^{(2)}, 1)}$	0.3995(14)	0.3636(38)	0.3300(58)	600(0)					
$H^{(O^{(w)}, 1)}$	0.2393(12)	0.6805(35)	0.4964(69)	600(0)					
$H^{(O^{(w)}, 2)}$	0.2919(13)	0.6866(38)	0.3329(63)	600(0)					
$H^{(S^{(1)}, 1)}$	0.4086(11)	−0.3022(32)	0.5494(61)	600(0)					

Table A.3. Point positions and thermal parameters of glycyl-L-leucine hydroiodide monohydrate, $C_8H_{19}IN_2O_4$. All atoms in position 2a of the space group $P2_1$: x, y, z; $\bar{x}, \frac{1}{2}+y, \bar{z}$. For definition of the temperature factor see Table A.1.

Atom	x/a	y/b	z/c	U_{11}, U	U_{22}	U_{33}	U_{12}	U_{13}	U_{23}
$I^{(1)}$	0.2090(0)	0.5000(0)	0.8773(0)	633(1)	342(1)	546(1)	−22(1)	87(1)	−24(1)
$C^{(1)}$	0.9495(2)	0.1931(3)	0.6522(5)	484(14)	247(11)	426(14)	−38(9)	71(12)	7(10)
$C^{(2)}$	0.8811(2)	0.3286(2)	0.6411(11)	427(11)	224(9)	344(11)	−2(8)	16(10)	15(9)
$C^{(3)}$	0.7235(2)	0.4352(3)	0.7436(4)	373(11)	309(11)	425(13)	−12(9)	5(10)	2(10)
$C^{(4)}$	0.6251(2)	0.3817(3)	0.8306(5)	425(14)	462(15)	572(18)	40(11)	119(13)	43(13)
$C^{(5)}$	0.5652(3)	0.2604(4)	0.6938(6)	484(16)	588(19)	768(24)	168(14)	72(16)	168(14)
$C^{(6)}$	0.4729(3)	0.2149(5)	0.8005(9)	691(26)	912(31)	1510(48)	340(22)	366(30)	155(31)
$C^{(7)}$	0.5285(5)	0.3030(7)	0.4640(7)	1661(52)	1638(54)	835(36)	1083(41)	−481(38)	−265(37)
$C^{(8)}$	0.7704(2)	0.5633(3)	0.8843(5)	386(12)	325(12)	567(17)	−23(9)	26(12)	−2(11)
$N^{(1)}$	1.0464(2)	0.2236(2)	0.5585(4)	472(13)	312(10)	488(14)	−71(9)	67(11)	40(10)
$N^{(2)}$	0.7997(2)	0.3183(2)	0.7470(4)	436(11)	266(10)	444(12)	−28(8)	101(10)	−72(9)
$O^{(1)}$	0.9001(2)	0.4374(2)	0.5389(3)	599(11)	288(8)	582(12)	−52(8)	299(10)	−107(8)
$O^{(2)}$	0.8407(1)	0.5568(2)	1.0353(4)	549(11)	449(11)	604(13)	−49(8)	−140(10)	89(9)
$O^{(3)}$	0.7208(2)	0.6854(2)	0.8159(5)	789(16)	336(11)	990(21)	−116(11)	−343(15)	134(12)
$O^{(w)}$	1.0082(2)	0.3434(2)	0.1372(4)	549(12)	503(12)	496(13)	−52(9)	109(11)	−30(10)
$H^{(C^{(3)}, 1)}$	0.7060(17)	0.4743(35)	0.5908(43)	600(0)					
$H^{(C^{(1)}, 1)}$	0.9696(27)	0.1723(39)	0.7839(59)	600(0)					
$H^{(C^{(1)}, 2)}$	0.9117(22)	0.1139(31)	0.5709(53)	600(0)					
$H^{(C^{(4)}, 1)}$	0.6486(22)	0.3519(31)	0.9704(52)	600(0)					
$H^{(C^{(4)}, 2)}$	0.5748(19)	0.4620(29)	0.8306(43)	600(0)					
$H^{(C^{(5)}, 1)}$	0.6122(22)	0.1657(31)	0.6936(52)	600(0)					
$H^{(C^{(6)}, 1)}$	0.4177(3)	0.3006(5)	0.8223(9)	600(0)					
$H^{(C^{(6)}, 2)}$	0.5071(3)	0.1724(5)	0.9593(9)	600(0)					
$H^{(C^{(6)}, 3)}$	0.4326(3)	0.1280(5)	0.7026(9)	600(0)					
$H^{(C^{(7)}, 1)}$	0.4866(5)	0.4055(7)	0.4424(7)	600(0)					
$H^{(C^{(7)}, 2)}$	0.4826(5)	0.2184(7)	0.3715(7)	600(0)					
$H^{(C^{(7)}, 3)}$	0.6030(5)	0.3138(7)	0.4057(7)	600(0)					
$H^{(N^{(1)}, 1)}$	1.0841(23)	0.1282(33)	0.5576(51)	600(0)					
$H^{(N^{(1)}, 2)}$	1.0823(27)	0.2718(39)	0.4136(56)	600(0)					
$H^{(N^{(1)}, 3)}$	1.0857(22)	0.2900(33)	0.6584(51)	600(0)					
$H^{(N^{(2)}, 1)}$	0.7948(20)	0.2549(30)	0.8095(46)	335(76)					
$H^{(O^{(3)}, 1)}$	0.7353(25)	0.7527(35)	0.8838(52)	600(0)					
$H^{(O^{(w)}, 1)}$	1.0496(24)	0.3925(32)	0.0781(56)	600(0)					
$H^{(O^{(w)}, 2)}$	0.9583(23)	0.3946(33)	0.1303(56)	600(0)					

Table A.4. Coefficients for the parameterization of the temperature dependence $\nu = f(T)$ according to $\nu = \sum_{i=-1}^{2} a_i \cdot T^i$.

Substance	NQR-signal	ΔT/K	m	σ/kHz [a]	$\frac{a_{-1}}{\text{MHz}\cdot\text{K}^{-1}}$	$\frac{a_0}{\text{MHz}}$	$\frac{10^3\, a_1}{\text{MHz}\cdot\text{K}}$	$\frac{10^6\, a_2}{\text{MHz}\cdot\text{K}^{-2}}$
L-Arg · HBr · H_2O	$\nu_1(^{79}Br)$	231–411	20	15	611.581	17.041	9.895	−20.782
	$\nu_2(^{81}Br)$	355–426	13	3	−1894.388	35.152	−38.802	27.006
	$\nu_2(^{79}Br)$	153–426	18	6	− 153.862	26.082	−6.407	−0.854
L-Cys · HBr · H_2O	$\nu(^{79}Br)$	77–337	19	3	10.578	13.873	2.769	2.489
L-Cys-S-S-L-Cys · 2 HBr	$\nu(^{79}Br)$	77–420	22	6	−28.974	24.352	−8.930	0.021
Ethanolamine · HBr	$\nu(^{79}Br)$	77–360	23	8	12.131	19.721	3.195	15.264
L-Glu · HBr	$\nu(^{79}Br)$	77–419	23	5	−13.473	13.173	−2.983	0.228
L-His · HBr	$\nu(^{79}Br)$	77–374	23	10	−45.716	22.650	−8.313	−0.486
L-His · 2 HBr	$\nu_1(^{79}Br)$	77–419	24	3	−12.862	19.037	−4.956	1.478
	$\nu_2(^{79}Br)$	77–417	24	5	−29.032	29.317	−7.032	−2.145
L-Ile · HBr · H_2O	$\nu(^{79}Br)$	273–316	6	2	−2610.297	41.001	−81.602	91.341
Sar · HBr	$\nu(^{79}Br)$	77–422	46	9	8.212	18.238	7.475	−8.265
Sar_2 · HBr	$\nu_1(^{79}Br)$	77–314	12	3	−5.413	17.947	−4.131	−12.323
	$\nu_2(^{79}Br)$	233–314	5	10	2219.217	−5.534	91.414	−141.179
L-Val · HBr · H_2O	$\nu(^{79}Br)$	273–320	6	6	3581.998	−18.982	117.491	128.957
Ethanolamine · HI	$\nu_1(^{127}I)$	77–345	20	14	27.089	17.303	4.276	−33.450
	$\nu_2(^{127}I)$	77–345	21	10	−8.047	22.424	−1.511	−39.293
Sar · HI (from solution)	$\nu_1^{I}(^{127}I)$	77–313	11	12	−70.544	25.340	−5.930	−31.720
Phase I	$\nu_2^{I}(^{127}I)$	77–314	12	16	77.740	40.098	−8.727	−23.878
(from melting)	$\nu_1^{II}(^{127}I)$	120–389	15	12	157.538	21.883	15.943	−31.814
Phase II	$\nu_2^{II}(^{127}I)$	253–374	7	5	−622.276	34.544	−20.209	1.436
Gyl_2 · HI	$\nu_1(^{127}I)$	163–374	16	8	110.508	20.141	−6.790	1.415
	$\nu_2(^{127}I)$	174–389	15	7	−73.640	23.223	−10.180	7.317
	$\nu_3(^{127}I)$	77–354	19	9	24.519	21.569	8.445	−26.299
	$\nu_4(^{127}I)$	77–389	21	10	46.327	23.838	9.400	−12.291
Sar_2 · HI	$\nu_1(^{127}I)$	77–314	12	2	−29.678	15.957	−13.059	21.089
	$\nu_2(^{127}I)$	77–314	12	12	−41.070	19.804	−1.323	−31.716
Gly-L-Leu · HI · H_2O	$\nu_1(^{127}I)$	77–306	47	4	39.312	22.668	3.419	−11.288
	$\nu_2(^{127}I)$	77–313	48	6	−67.101	29.006	−6.413	−18.101

[a] Mean error $\sigma = \left(\frac{\sum (\nu_{meas} - \nu_{calc})^2}{m-n}\right)^{1/2}$; m = number of measurements $\nu = f(T)$, n = number of parameters in the power series.

Table A.5. Comparison of ^{79}Br NQR frequencies at $T = 273$ K and hydrogen bond coordination of the bromine ion.

Nr.	Compound	$\nu(^{79}Br)$/MHz ($T = 273$ K)	Coordination of $Br^{\ominus}$	Literature NQR; Structure
1. N–H ··· $Br^{\ominus}$ bonds only				
1	$MeNH_2$ · HBr	12.950 [a]	4 × N–H ··· $Br^{\ominus}$	[65]; [66, 65]
2	Me_2H · HBr	13.71 [b]	3 × N–H ··· $Br^{\ominus}$	[67]
3	Me_3N · HBr	18.40 [b]	N–H ··· $Br^{\ominus}$	[67]; [68]
4	$EtNH_2$ · HBr	18.700	3 × N–H ··· $Br^{\ominus}$	[65]; [69, 65]
5	Et_2NH · HBr	16.48 [b]	N–H ··· $Br^{\ominus}$	[67]
6	Et_3N · HBr	14.43 [b]	N–H ··· $Br^{\ominus}$	[67]
7	n-$C_3H_7NH_2$ · HBr	12.01 [b]	N–H ··· $Br^{\ominus}$	[67]; [70]
9	Gly_2 · HBr	17.340	3 × N–H ··· $Br^{\ominus}$	[1]; [71]
11	Sar_2 · HBr	15.845	3 × N–H ··· $Br^{\ominus}$	[c]; [54]
		17.013	3 × N–H ··· $Br^{\ominus}$	
23	His · 2 HBr	17.751	2 × N–H ··· $Br^{\ominus}$	[c]; [c]
29	Gly-L-Ala · HBr · H_2O	13.735	3 × N–H ··· $Br^{\ominus}$	[4]; [72]
31	4-$ClC_6H_4NH_2$ · HBr · 1/2 H_2O	19.134	3 × N–H ··· $Br^{\ominus}$	[2]; [2]
32	4-$BrC_6H_4NH_2$ · HBr · 1/2 H_2O	18.164	3 × N–H ··· $Br^{\ominus}$	[2]; [2]

Table A.5.

Nr.	Compound	$\nu(^{79}Br)$/MHz ($T = 273$ K)	Coordination of $Br^{\ominus}$	Literature NQR; Structure
2. N–H ··· $Br^{\ominus}$ bonds and one O–H ··· $Br^{\ominus}$ bond				
8	$HOC_2H_4NH_2 \cdot HBr$	19.500	$1 \times O–H \cdots Br^{\ominus}$, $3 \times N–H \cdots Br^{\ominus}$	[c]; [47]
15	Leu · HBr	25.606	$1 \times O–H \cdots Br^{\ominus}$, $3 \times N–H \cdots Br^{\ominus}$	[1]; [29]
20	Cys-S-S-Cys · 2 HBr	21.809	$1 \times O–H \cdots Br^{\ominus}$, $3 \times N–H \cdots Br^{\ominus}$	[c]; [42]
21	Arg · HBr · H_2O	20.435	$1 \times O–H \cdots Br^{\ominus}$, $3 \times N–H \cdots Br^{\ominus}$	[c]; [35]
		23.705	$1 \times O–H \cdots Br^{\ominus}$, $3 \times N–H \cdots Br^{\ominus}$	
23	His · 2 HBr	27.130	$1 \times O–H \cdots Br^{\ominus}$, $2 \times N–H \cdots Br^{\ominus}$	[c]; [c]
3. Two N–H ··· $Br^{\ominus}$ bonds and two O–H ··· $Br^{\ominus}$ bonds				
31	$4\text{-}ClC_6H_4NH_2 \cdot HBr \cdot 1/2\ H_2O$	13.512	$2 \times O–H \cdots Br^{\ominus}$, $2 \times N–H \cdots Br^{\ominus}$	[2]; [2]
32	$4\text{-}BrC_6H_4NH_2 \cdot HBr \cdot 1/2\ H_2O$	13.948	$2 \times O–H \cdots Br^{\ominus}$, $2 \times N–H \cdots Br^{\ominus}$	[2]; [2]
4. Three O–H ··· $Br^{\ominus}$ bonds and one N–H ··· $Br^{\ominus}$ bond				
16	Ile · HBr · H_2O	15.970	$3 \times O–H \cdots Br^{\ominus}$, $1 \times N–H \cdots Br^{\ominus}$	[c]; [32]
19	Cys · HBr · H_2O	14.862	$3 \times O–H \cdots Br^{\ominus}$, $1 \times N–H \cdots Br^{\ominus}$	[c]; [c]
5. Compounds with unknown crystal structure				
10	Gly · HBr	25.365		[1]
12	Sar · HBr	17.875		[c]
13	Ala · HBr	25.764		[1]
18	Pro · HBr	18.661		[1]
22	His · HBr	20.172		[c]
24	Asp · HBr	26.397		[4]
25	Glu · HBr	12.320		[c]
26	Asn · HBr · 1/2 H_2O	20.475		[4]
27	Trp · HBr	23.119		[53]
28	GlyGly · HBr · H_2O	12.419		[4]

[a] $T = 293$ K. [b] $T = 303$ K. [c] This work.

Table A.6. Comparison of nuclear quadrupole coupling constants $e\Phi_{zz}Qh^{-1}(^{127}I)$ at 273 K and hydrogen bond coordination of the iodine ion.

No.	Compound	$e\Phi_{zz}Qh^{-1}(^{127}I)$ MHz ($T = 273$ K)	Coordination of $I^{\ominus}$	Literature NQR; Structure
1. N–H ··· $I^{\ominus}$ bonds only				
1	$MeNH_2 \cdot HI$	89.13 [a]	$4 \times N–H \cdots I^{\ominus}$	[65]; [66, 65]
3	$Me_3N \cdot HI$	123.74 [b]	$1 \times N–H \cdots I^{\ominus}$	[67]; [73]
4	$EtNH_2 \cdot HI$	112.15 [a]	$3 \times N–H \cdots I^{\ominus}$	[65]; [69, 65]
5	$Et_2NH \cdot HI$	110.17 [b]	$N–H \cdots I^{\ominus}$	[67]
7	$n\text{-}C_3H_7NH_2 \cdot HI$	79.89 [b]	$N–H \cdots I^{\ominus}$	[67]
9	$Gly_2 \cdot HI$	76.02 –	$4 \times N–H \cdots I^{\ominus}$	[c]; [58]
		91.83	$4 \times N–H \cdots I^{\ominus}$	
25	Glu · HI	82.11	$2 \times N–H \cdots I^{\ominus}$	[4]; [52]
29	Gly-L-Ala · HI · H_2O	74.04	$3 \times N–H \cdots I^{\ominus}$	[62]; [62]
2. N–H ··· $I^{\ominus}$ bonds and one OH ··· $I^{\ominus}$ bond				
15	Leu · HI	155.67	$1 \times O–H \cdots I^{\ominus}$, $2 \times N–H \cdots I^{\ominus}$	[1]; [30]
3. Two N–H ··· $I^{\ominus}$ bonds and two O–H ··· $I^{\ominus}$ bonds				
30	Gly-L-Leu · HI · H_2O	94.87	$2 \times O–H \cdots I^{\ominus}$, $2 \times N–H \cdots I^{\ominus}$	[c]; [c]
4. Compounds with unknown crystal structure				
11	$Sar_2 \cdot HI$	61.72		[c]
12	Sar · HI Phase I	122.08		[c]
	Phase II	98.91		[c]
14	$Val_2 \cdot HI$	138.40 [d]		[c]
17	Phe · HI	144.57 [d]		[c]
26	Asn · HI · H_2O	123.47		[4]
28	GlyGyl · HI · H_2O	73.00		[4]

[a] $T = 293$ K.
[b] $T = 300$ K.
[c] This work.
[d] Room temperature.